Search for cosmological phase transitions through their gravitational wave signals

Marek Lewicki

University of Warsaw

Oscar Klein Centre, University of Stockholm, 7 XI 2024

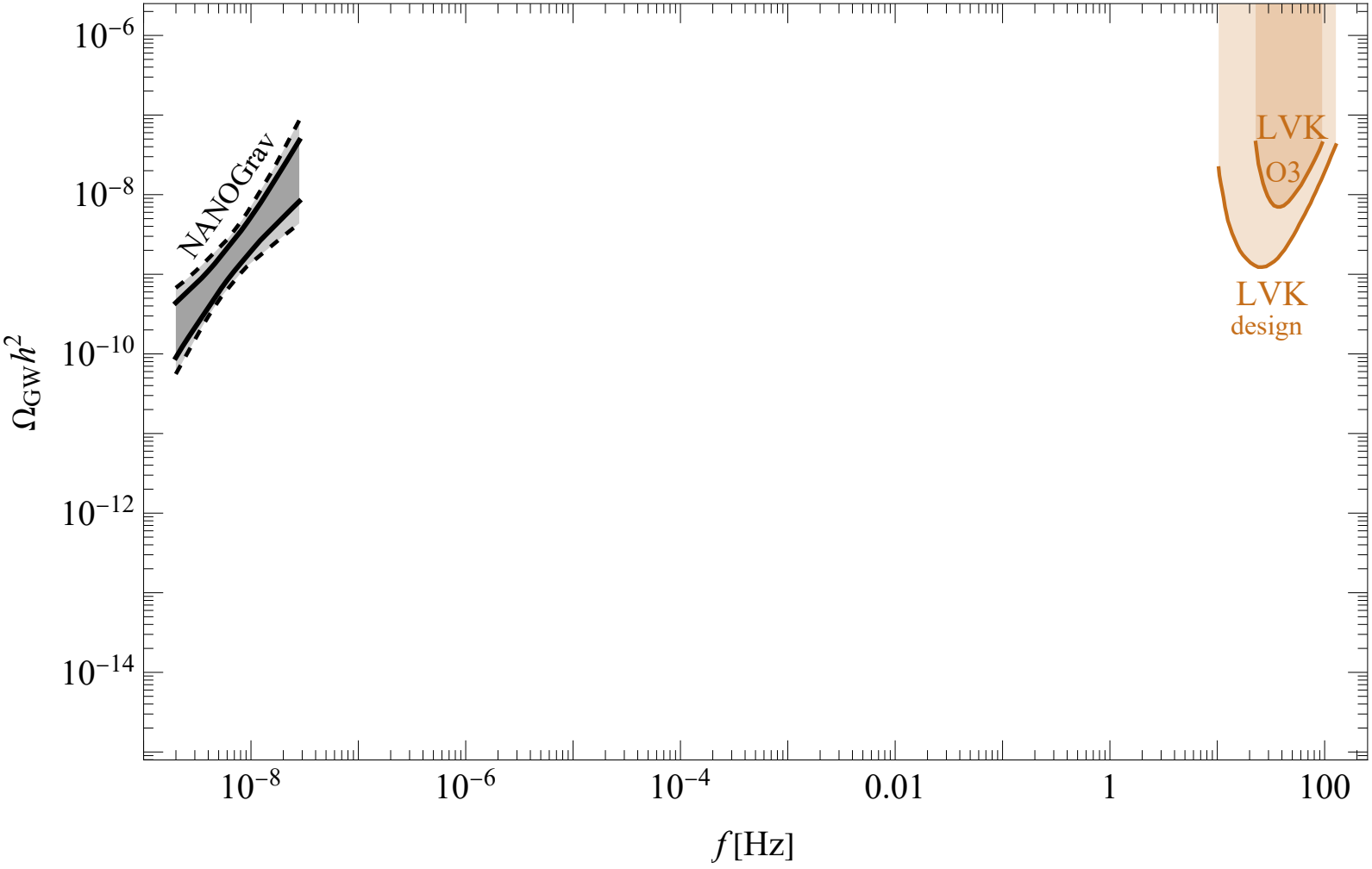
10^{-6}
10^{-8}
10^{-10}
10^{-12}
10^{-14}
$\Omega_{\rm GW}h^2$
NANOGrav
LVK
O3
LVK
design
10^{-8}
10^{-6}
10^{-4}
0.01
1
100
f[Hz]

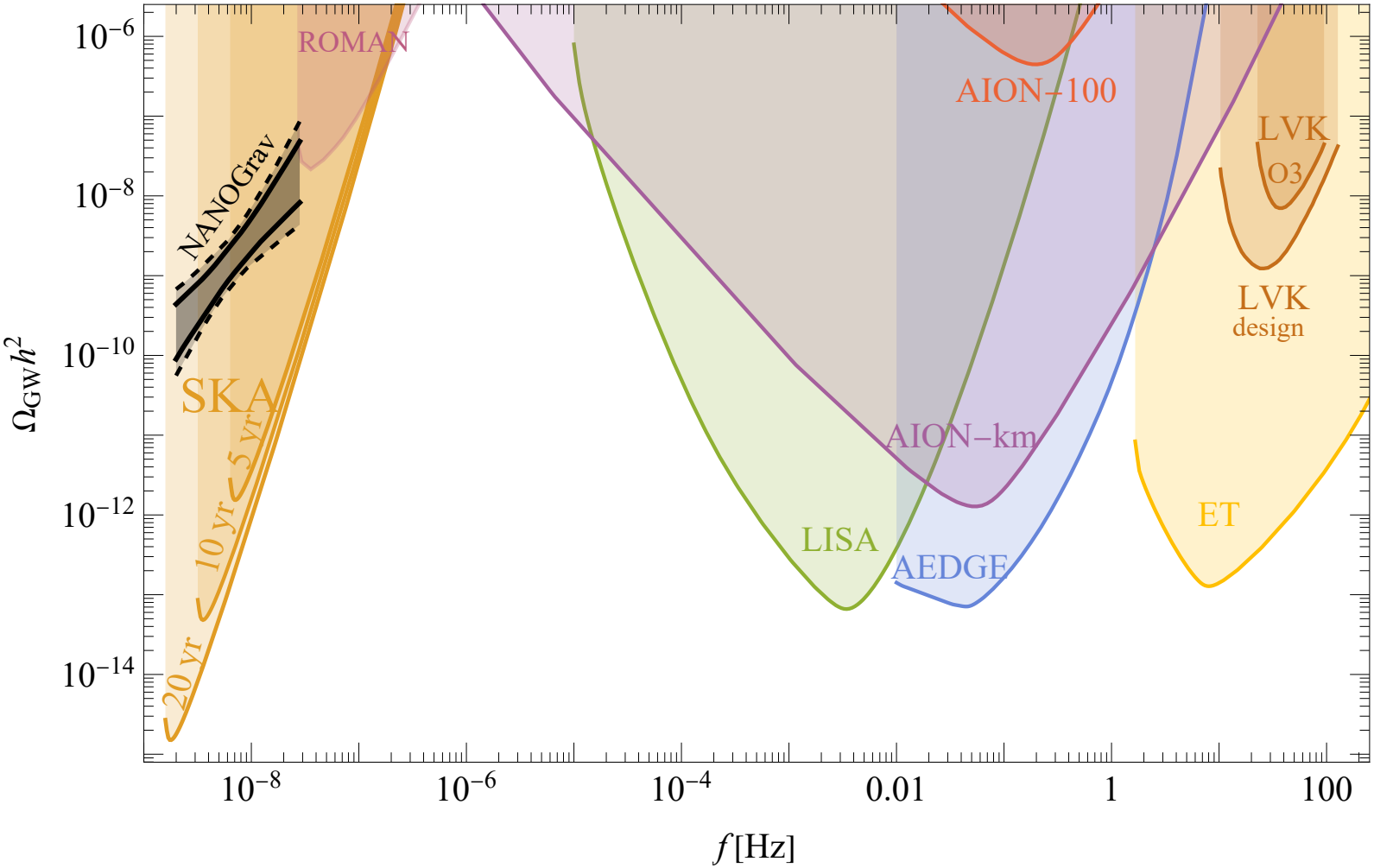

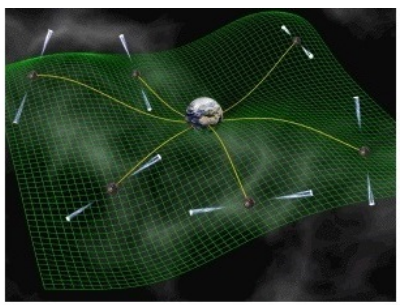

Pulsar Timing

[David Champion/NASA/JPL]

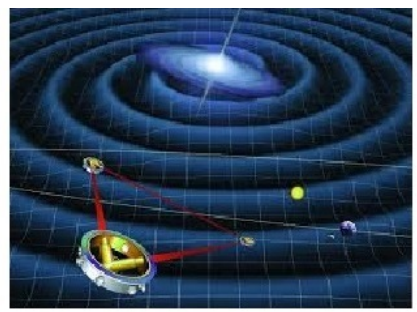

LISA

wiki/Laser_Interferometer_Space_Antenna

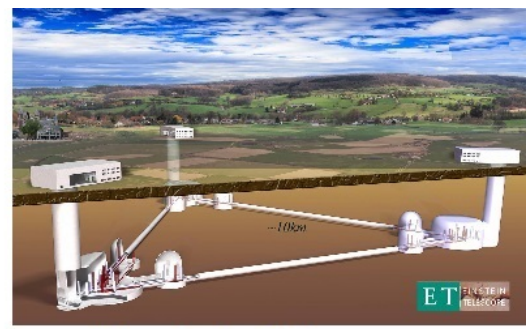

Einstein Telescope

www.et-gw.eu

Sensitivity to binary mergers

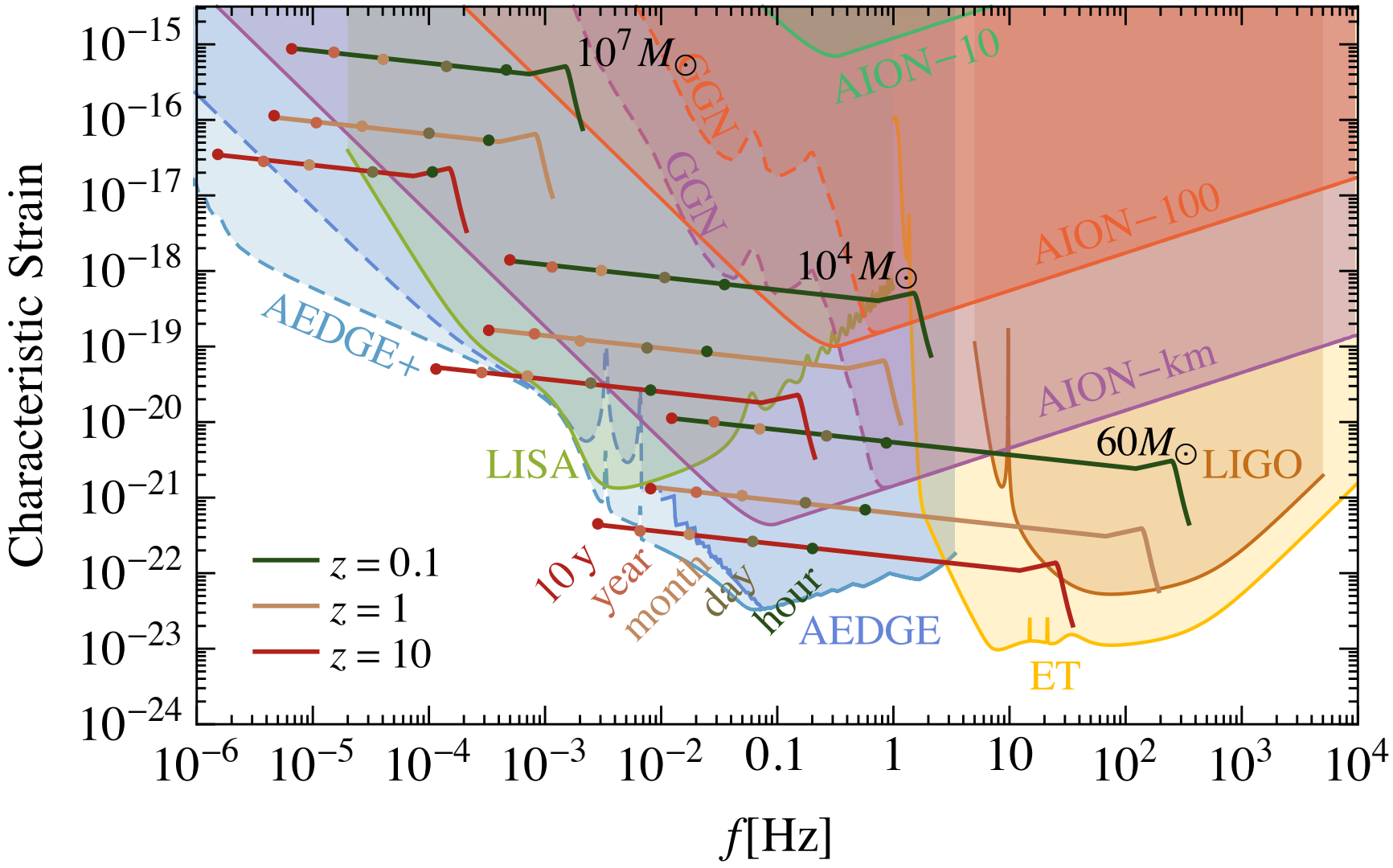

Foreground from LIGO-Virgo binaries

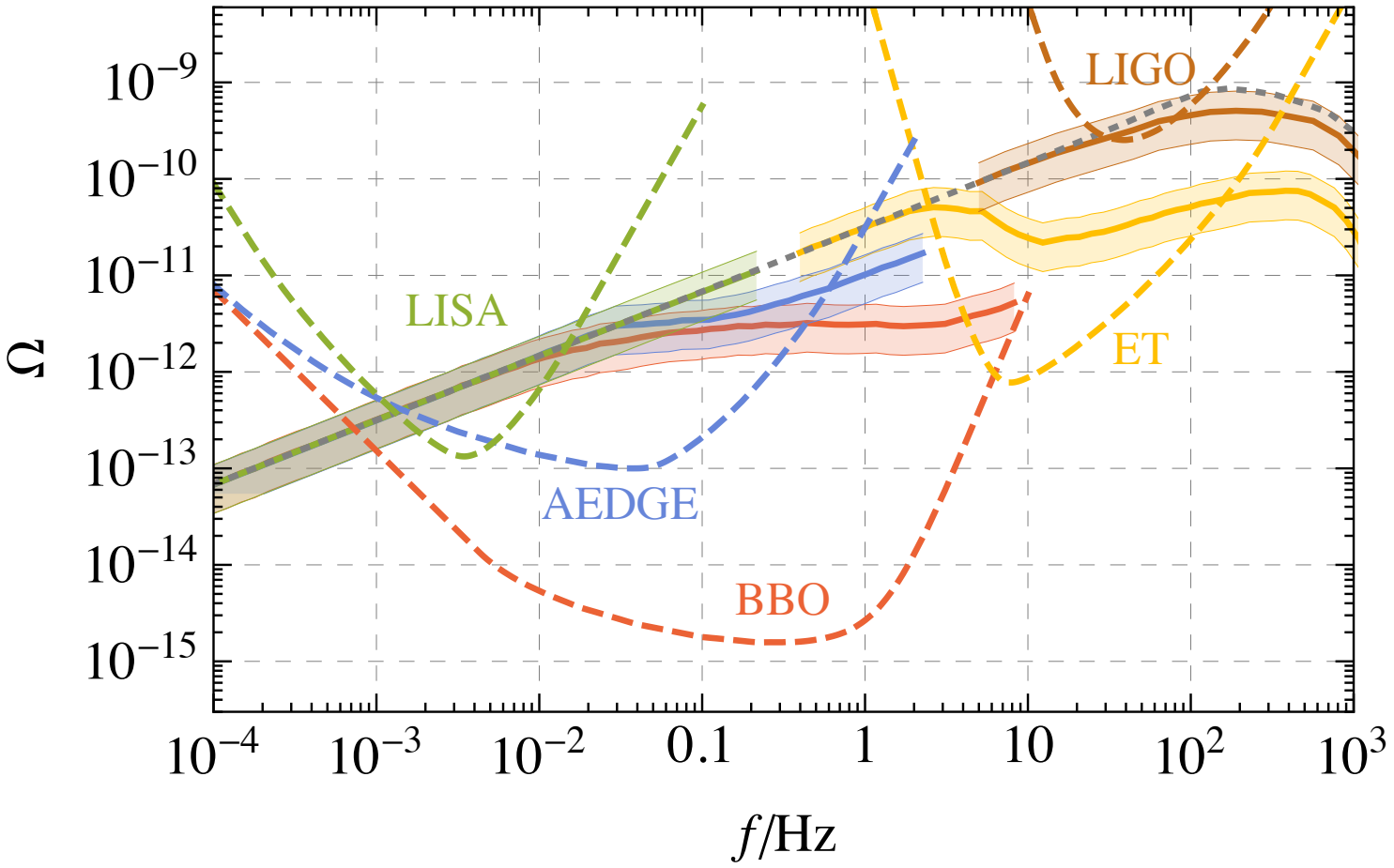

- Dashed gray line: total foreground from LIGO-Virgo binaries
- Thick lines: foreground without individually observable binaries

ML, Ville Vaskonen arXiv:2111.05847

Improved sensitivities from Fisher analysis

- assuming power-law signal as in PI sensitivity

$$\Omega_{\rm GW}(f) = \Omega \left(\frac{f}{f_{\rm ref}}\right)^{\alpha} + A\langle\Omega_{\rm BBH}(f)\rangle + \Omega_{\rm BWD}(f) + \Omega_{\rm instr}(f)$$

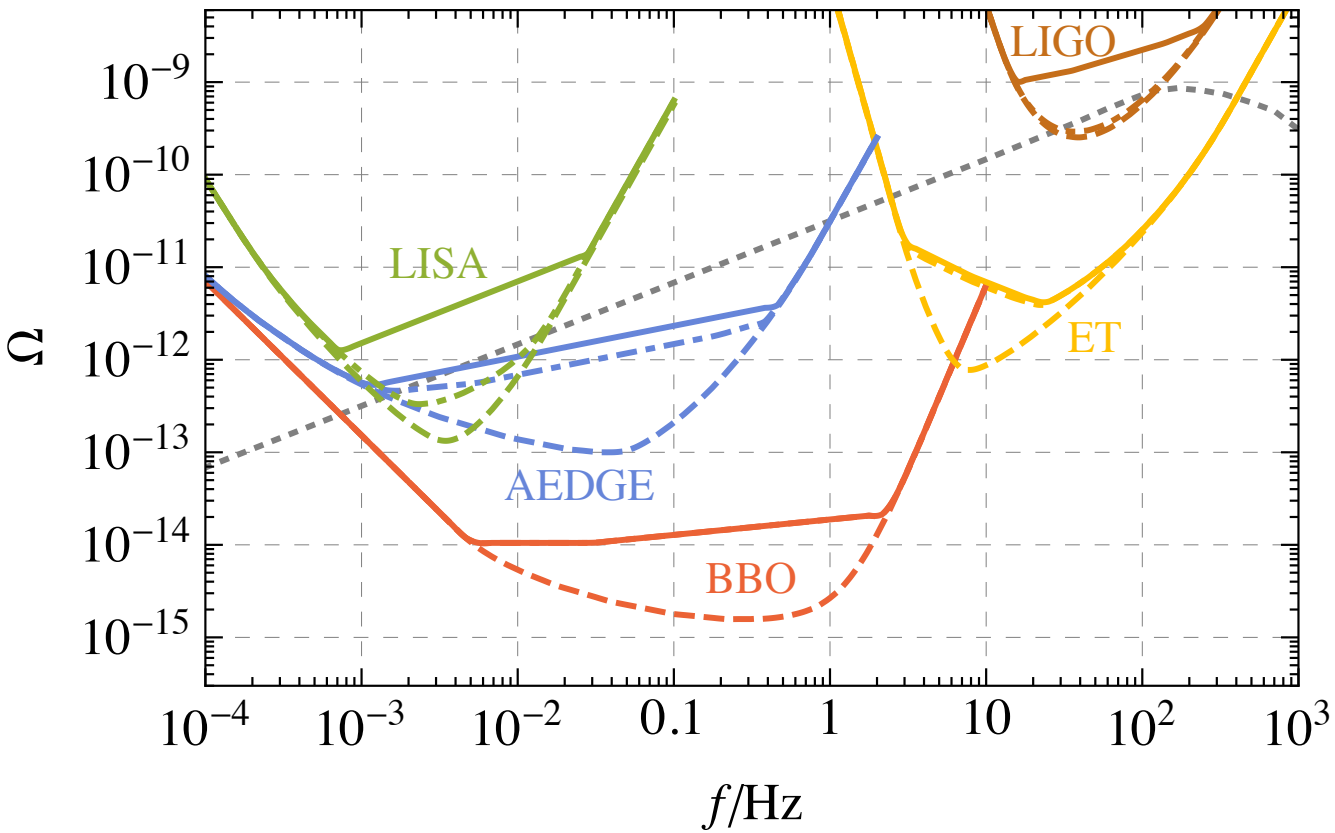

ML, Ville Vaskonen arXiv:2111.05847

Early Universe Sources

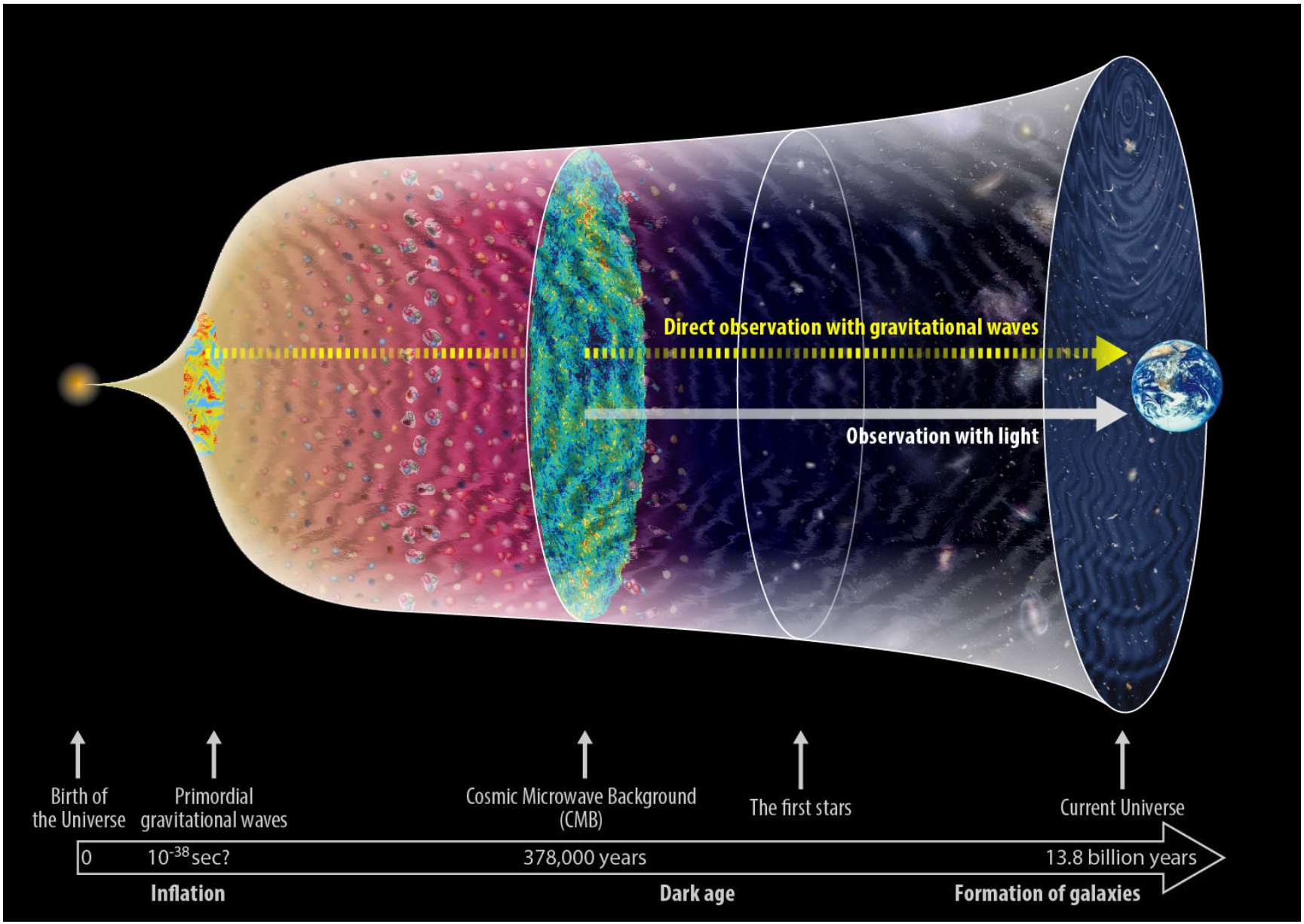

plot credit:https://gwpo.nao.ac.jp/en/gallery

First Order Phase Transition: bubble nucleation

- Temperature corrections to the potential

$$V(\phi, T) = \frac{g_m{}^2}{24}\left(T^2 - T_0^2\right)\phi^2 - \frac{g_m}{12\pi}T\phi^3 + \lambda\phi^4$$

- EOM $\rightarrow$ bubble profile

$$\frac{d^2\phi}{dr^2} + \frac{2}{r}\frac{d\phi}{dr} - \frac{\partial V(\phi, T)}{\partial\phi} = 0,$$

$$\phi(r \to \infty) = 0 \quad \text{and} \quad \dot{\phi}(r = 0) = 0.$$

- $\mathcal{O}(3)$ symmetric action

$$S_3(T) = 4\pi \int dr r^2 \left[\frac{1}{2}\left(\frac{d\phi}{dr}\right)^2 + V(\phi, T)\right].$$

- nucleation temperature

$$\frac{\Gamma}{H^4} \approx \left(\frac{T}{H}\right)^4 \exp\left(-\frac{S_3(T)}{T}\right) \approx 1$$

Linde '81 '83

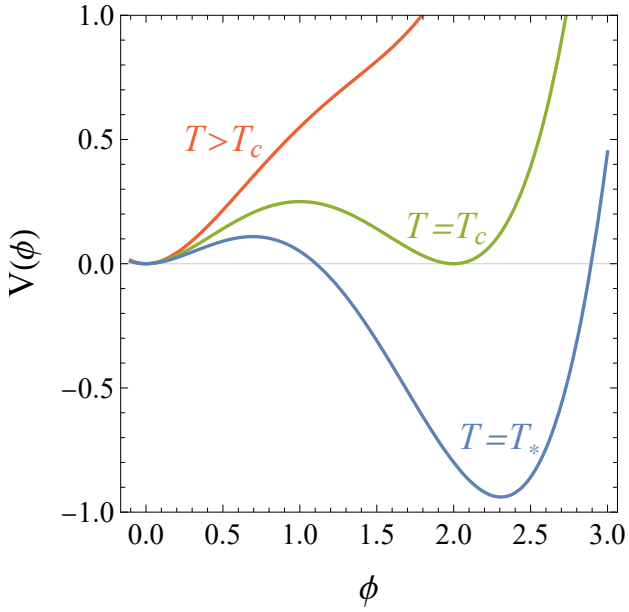

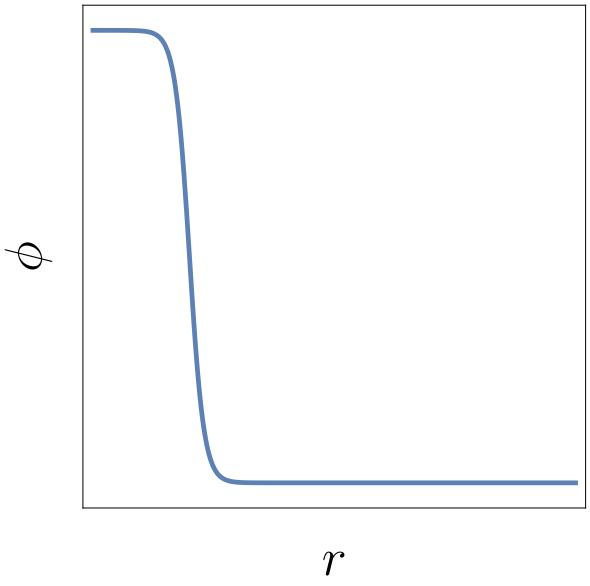

Gravitational waves from a PT

- Strength of the transition

$$\alpha \approx \left. \frac{\Delta V - T \frac{d\Delta V}{dT}}{\rho_R} \right|_{T=T_*}, \quad \Delta V = V_f - V_t$$

- Characteristic scale

$$\Gamma \propto e^{-\frac{S_3(T)}{T}} = e^{\beta\,(t-t_0)} \Longrightarrow \frac{\beta}{H} = T \frac{d}{dT} \left(\frac{S_3(T)}{T} \right) \Bigg|_{T=T_*}$$

- Peak frequency

$$f_p \propto T_* \frac{\beta}{H}$$

Three main sources of GWs

- collisions of bubble walls

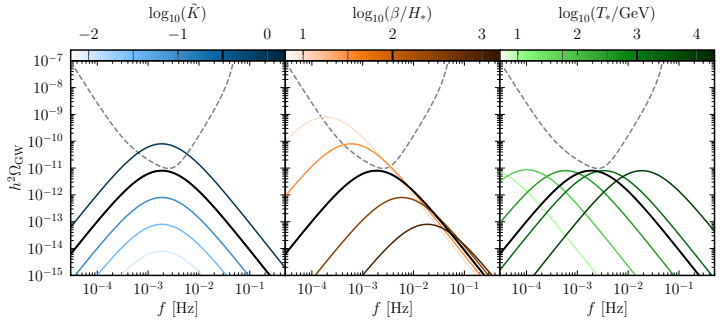

- sound waves

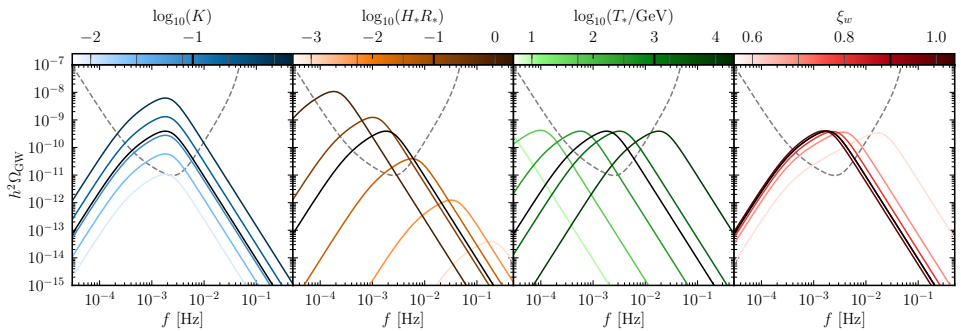

- turbulence

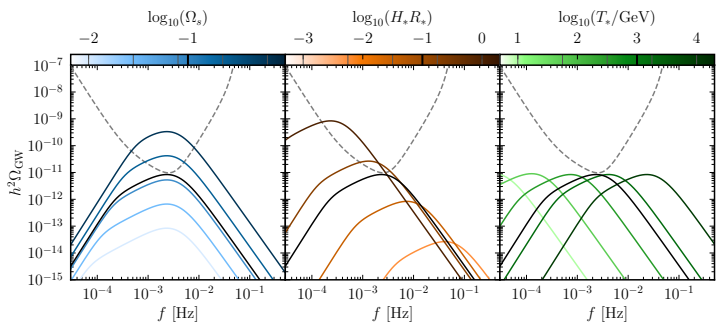

LISA Cosmology Working Group, arXiv: 2403.03723

Sound Waves (in weak transitions $\alpha \lesssim 0.1$)

- Simulation of a scalar coupled to the plasma

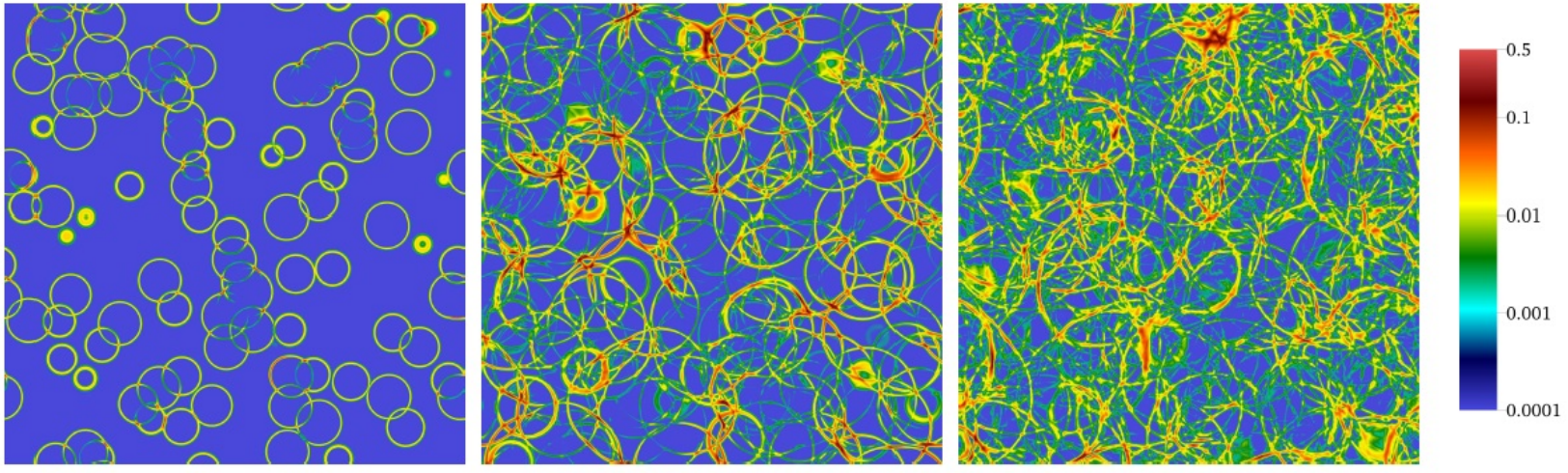

FIG. 4. Slices of fluid kinetic energy density E/T_c^4 at $t = 500\,T_c^{-1}$, $t = 1000\,T_c^{-1}$ and $t = 1500\,T_c^{-1}$ respectively, for the $\eta/T_c = 0.15$, $N_b = 988$ simulation.

- Fit to the GW spectrum

$$\Omega_{\rm gw} \propto \left(\frac{f}{f_p}\right)^3 \left(\frac{7}{4+3\,(f/f_p)^2}\right)^{\frac{7}{2}}$$

Hindmarsh, Huber, Rummukainen, Weir, arXiv: 1504.03291, 1704.05871

Sound Waves (in weak transitions $\alpha \lesssim 0.1$)

- Higgsless simulation of the plasma

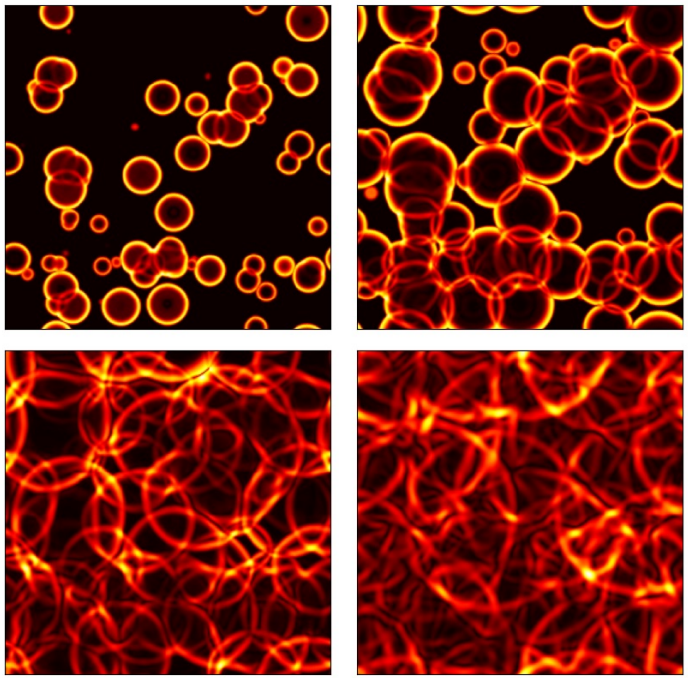

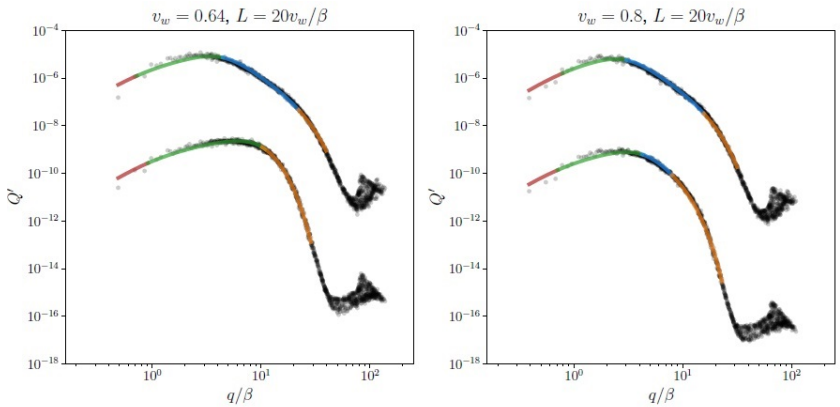

Figure 4: Kinetic energy v^2 in different simulation snapshots: $t = 2.7/\beta$ (top left), $5.4/\beta$ (top right), $10.8/\beta$ (bottom left) and $20.1/\beta$ (bottom right). We use box size $L = 40v_w/\beta$, weak transitions and $v_w = 0.8$.

- Fit to the GW spectrum

$$\Omega_{\rm gw} \propto \frac{(f/f_1)^3}{1 + (f/f_1)^2[1 + (f/f_2)^4]}, \qquad f_2/f_1 \approx 1/\xi_{\rm shell}$$

Jinno, Konstandin, Rubira, Stomberg, arXiv: 2209.04369

Sound Waves (in less weak transitions $\alpha \lesssim 0.5$)

- Higgsless simulation of the plasma

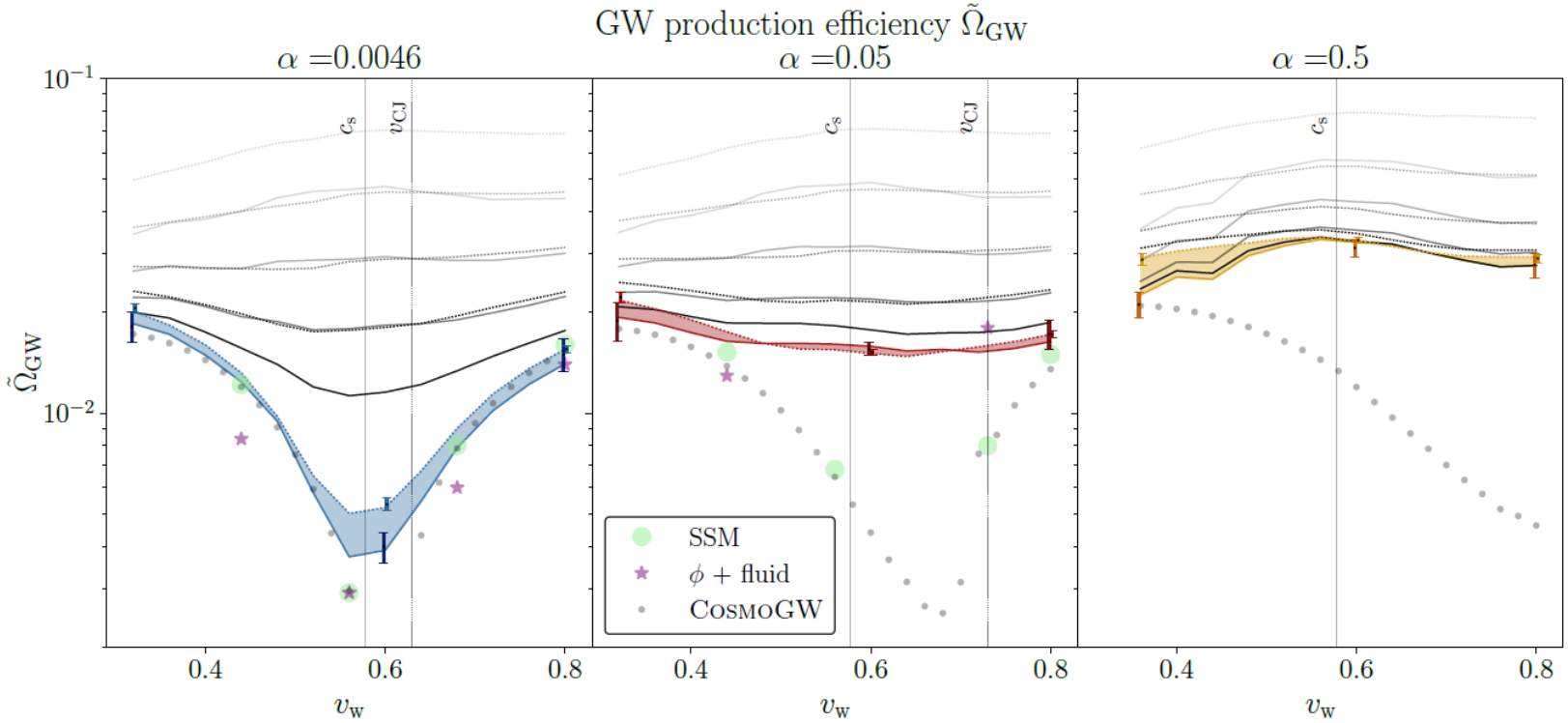

- Fit to the GW spectrum unchanged

$$\Omega_{\rm gw} \propto \frac{(f/f_1)^3}{1+(f/f_1)^2[1+(f/f_2)^4]}, \qquad f_2/f_1 \approx 1/\xi_{\rm shell}$$

Caprini, Jinno, Konstandin, Roper-Pol, Rubira, Stomberg, arXiv: 2409.03651

Gravitational waves from a very strong PT

- Strength of the transition

$$\alpha \approx \frac{\Delta V}{\rho_R} \gg 1$$

- Reheating temperature

$$T_{\rm reh} \approx \left(\frac{30}{\pi^2} \frac{1}{g_*} \Delta V \right)^{\frac{1}{4}}$$

- Characteristic scale

$$\Gamma \propto e^{-\frac{S_3(T)}{T}} = e^{\beta\,(t-t_0)} \Longrightarrow \frac{\beta}{H} = T \frac{d}{dT} \left(\frac{S_3(T)}{T} \right) \Big|_{T=T_p}$$

- Amplitude of the spectrum

$$\Omega_{\rm p} \propto \left(\frac{\alpha}{\alpha + 1} \right)^2 \left(\frac{\beta}{H} \right)^{-2}$$

- Peak frequency

$$f_p \propto T_{\rm reh} \frac{\beta}{H}$$

Strong transitions: computation of the GW spectrum

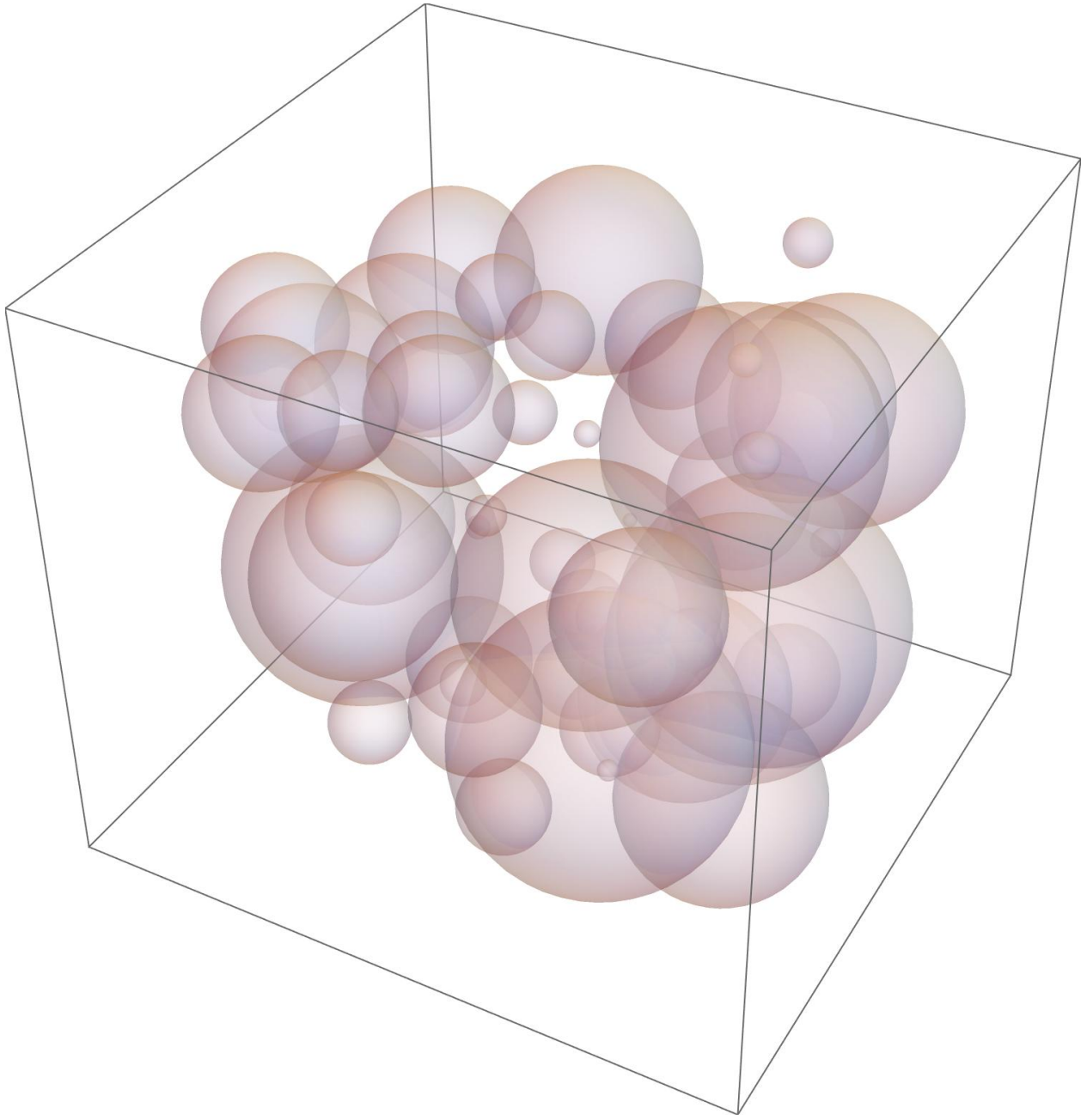

Bubble Collisions

- Envelope

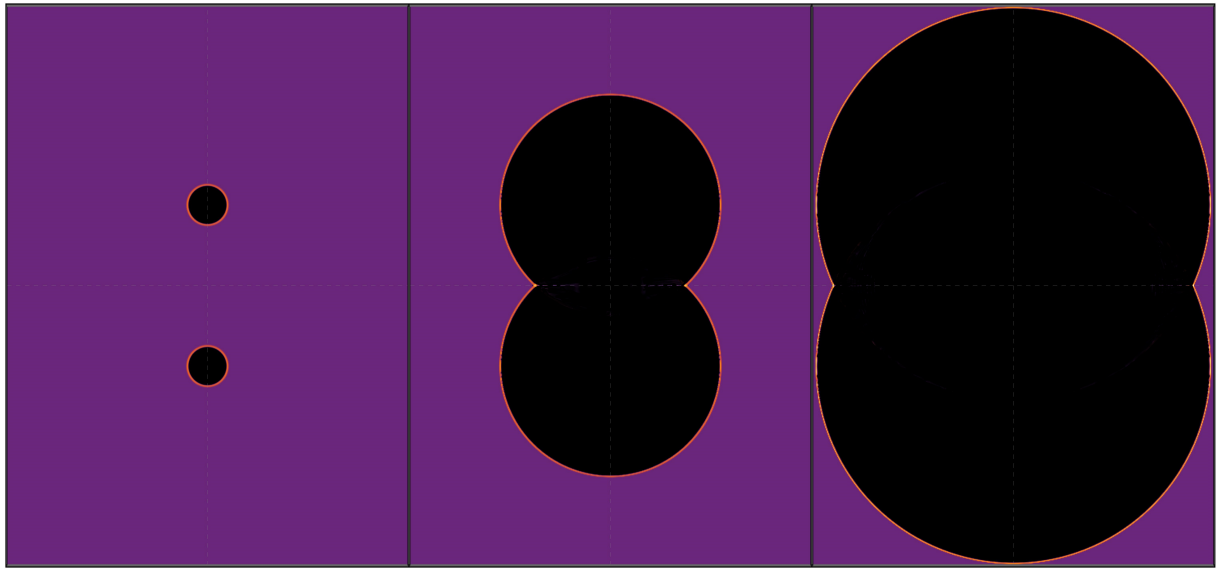

Bubble Collisions

- Envelope

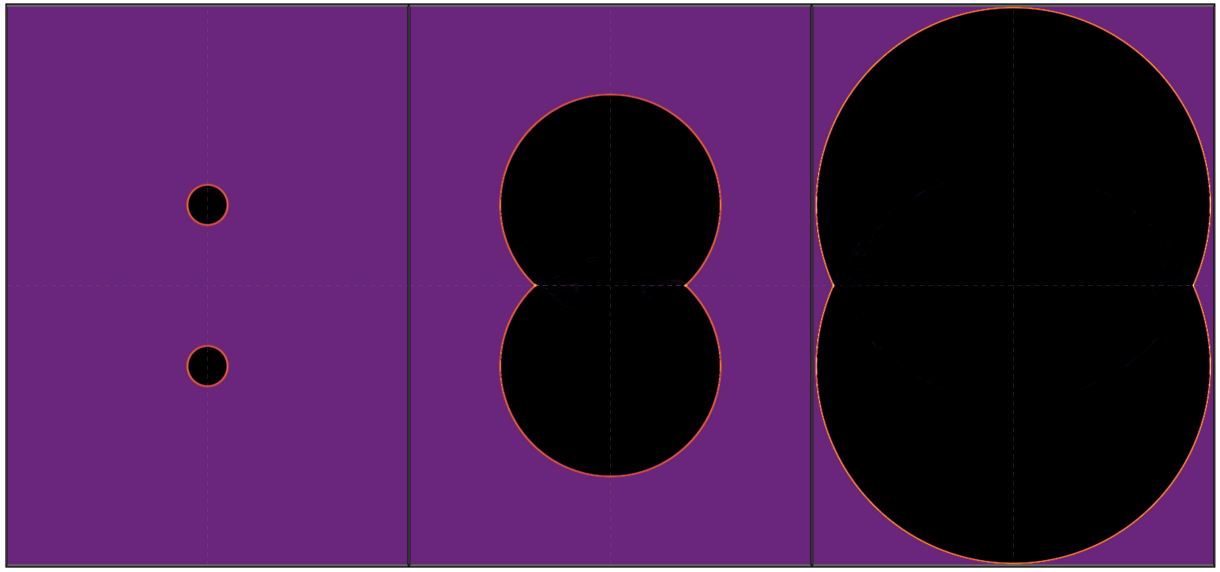

- Simulation

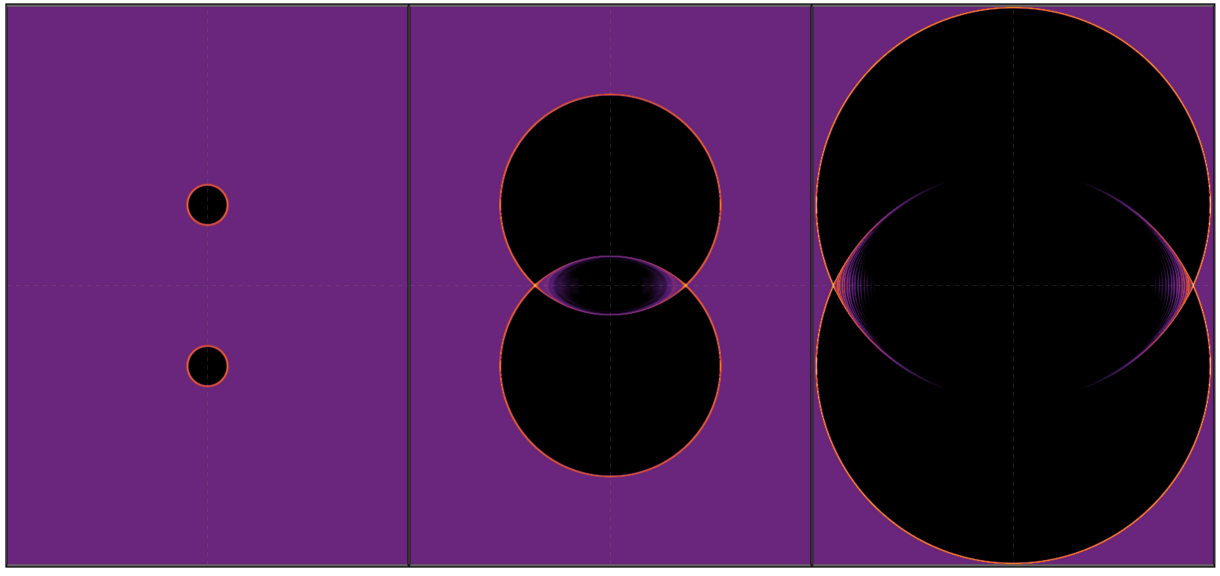

Vacuum Trapping

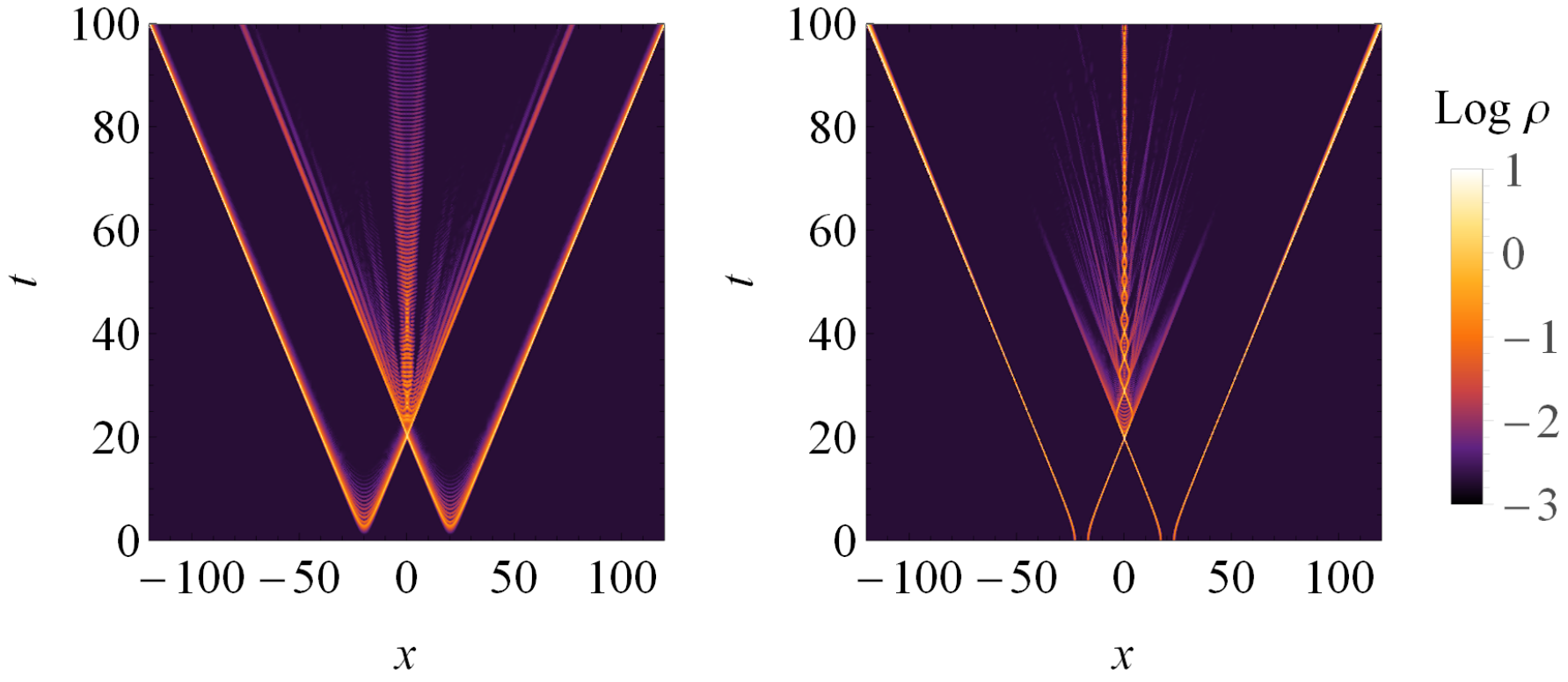

Vacuum Trapping

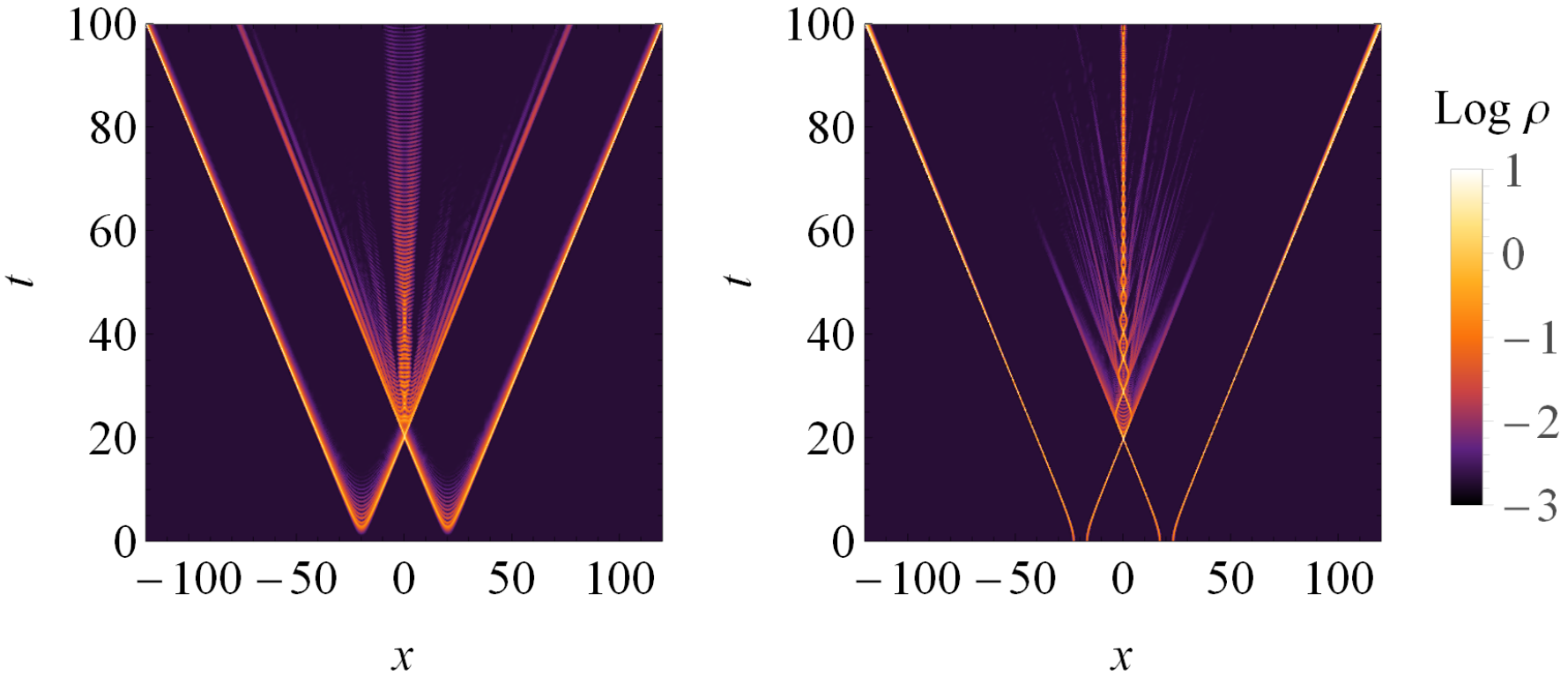

- scale-invariant vs. polynomial

- can also be verified analytically:
  R. Jinno, T. Konstandin and M. Takimoto: 1906.02588

Abelian Higgs Model: Energy Scaling

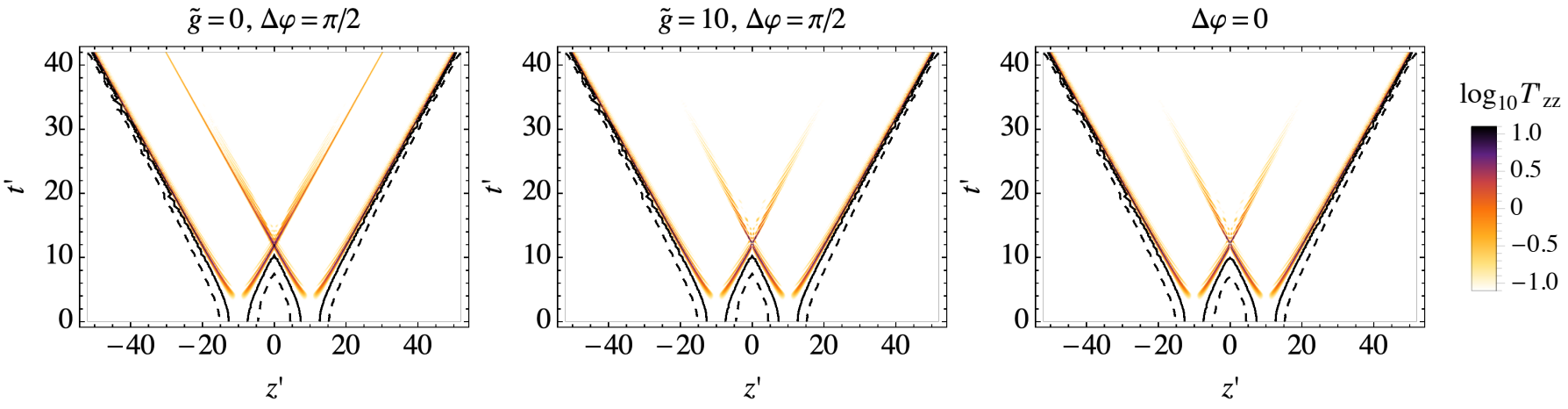

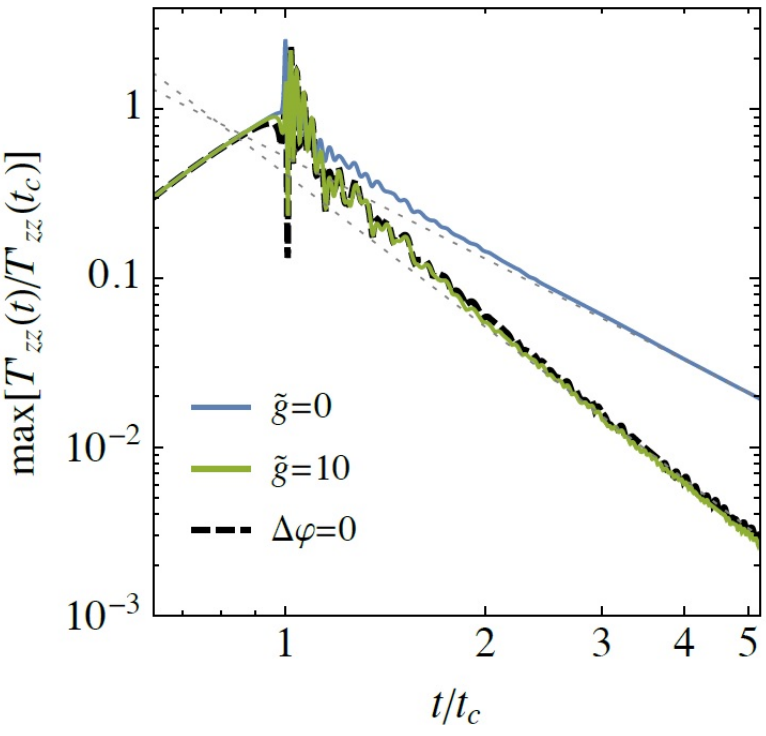

- scaled gauge coupling:

$$\tilde{g} = \frac{gv^2}{\sqrt{\Delta V}}$$

- Global Symmetry breaking:

$$T_{zz} \propto R^{-2}$$

- Gauge Symmetry breaking:

$$T_{zz} \propto R^{-3}$$

ML, Ville Vaskonen arXiv: 2007.04967

Fluid Shells in strong transitions

- Plasma profiles for $v_w \gtrsim v_J$

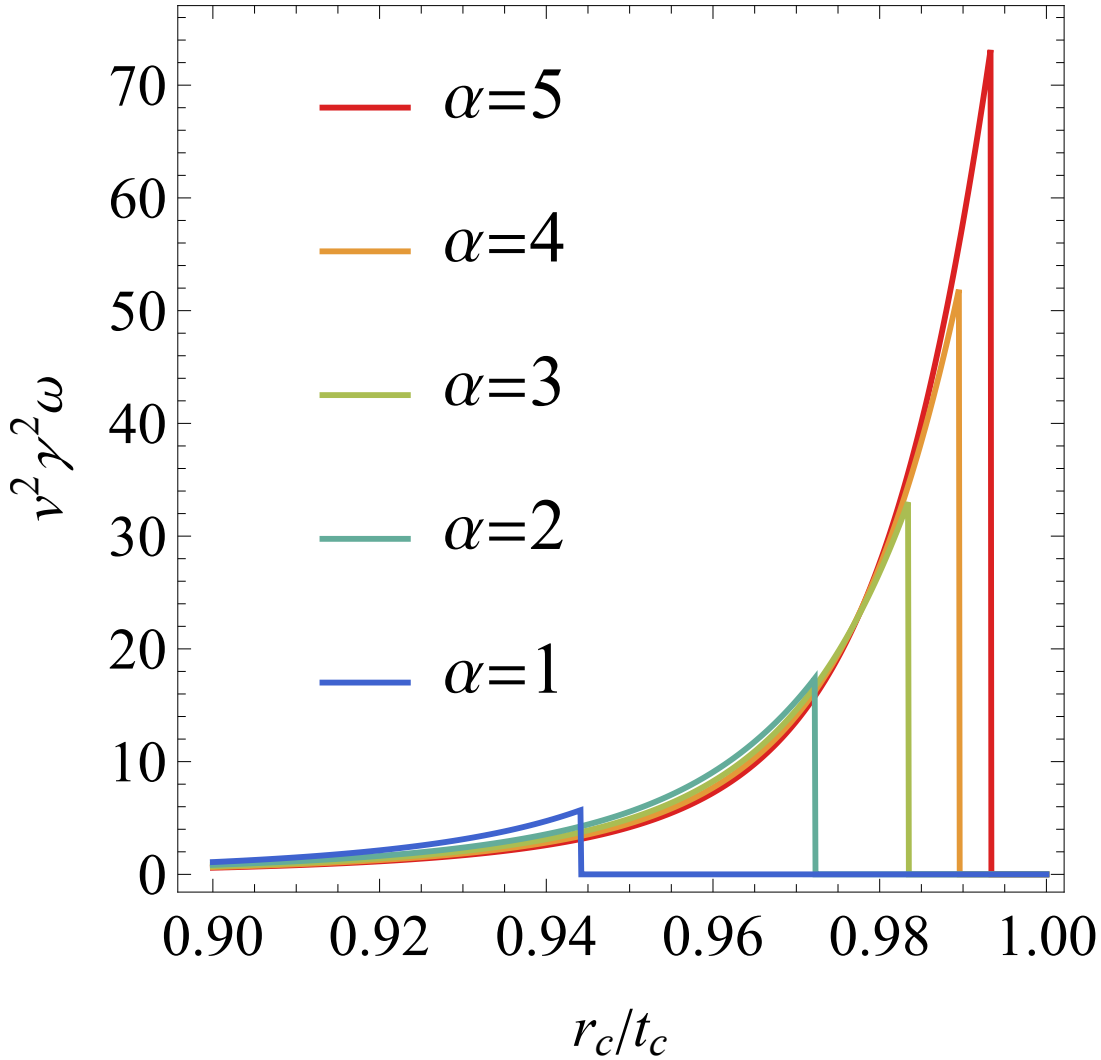

Fluid Shell Evolution

- Plasma profile evolution with $\alpha = 20$ and $\gamma_w = 50$

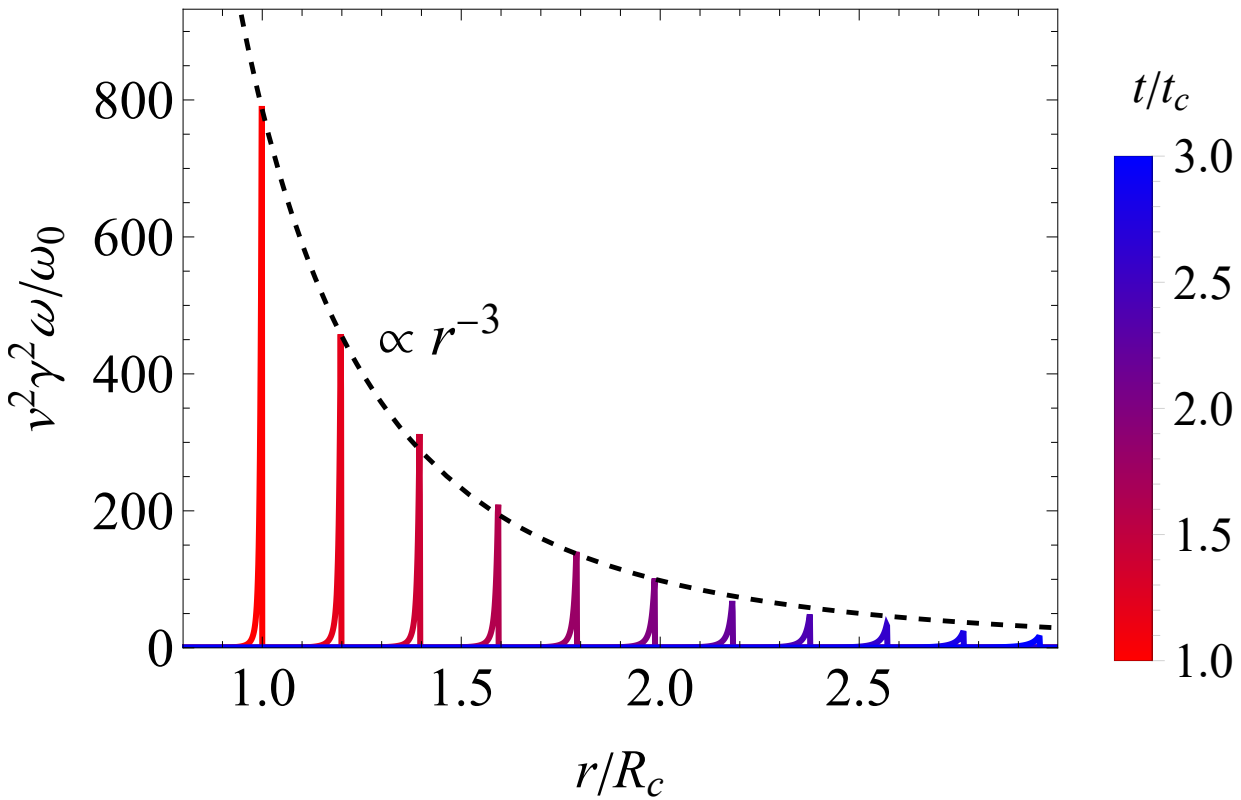

- Fluid shells with $\alpha \gg 1$:

$$T_{zz} \propto R^{-3}$$

ML, Ville Vaskonen arXiv:2208.11697

Fluid Shell Evolution

- Plasma profile evolution with $\alpha = 0.5$ and $\gamma_w = 3$

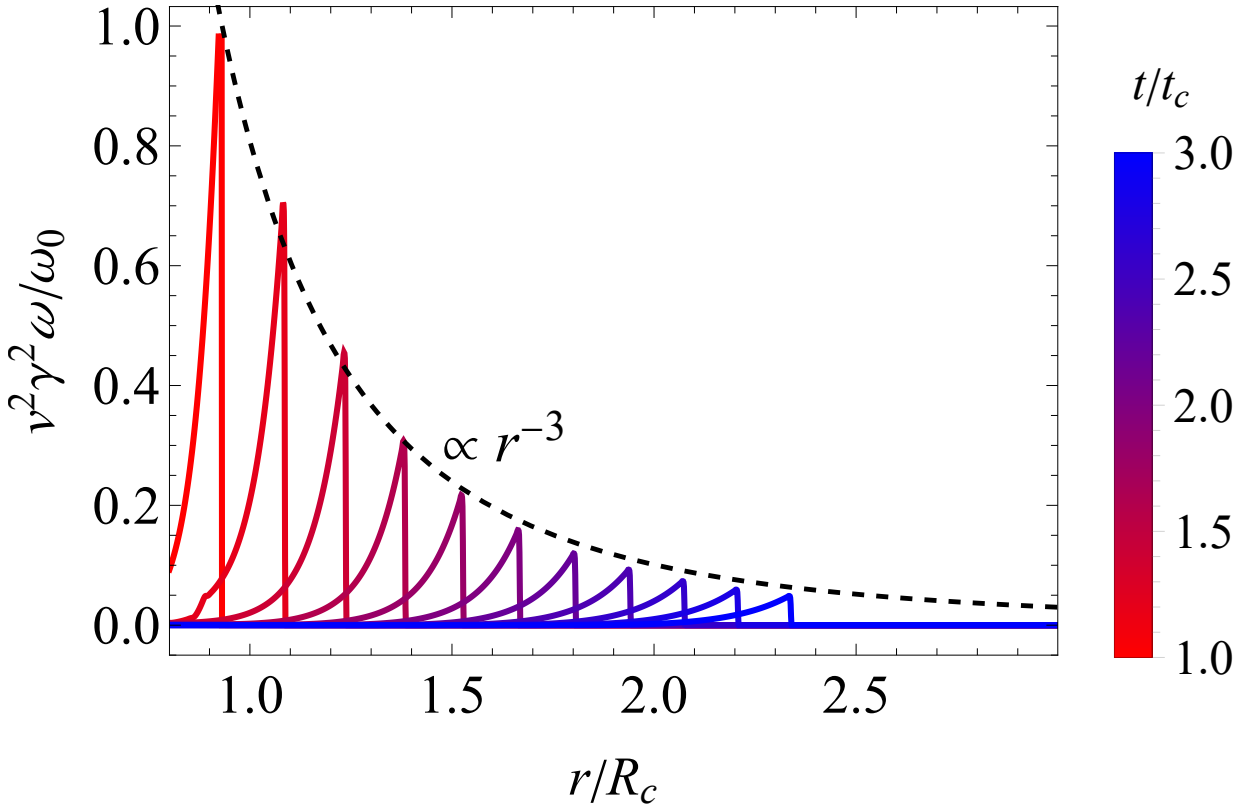

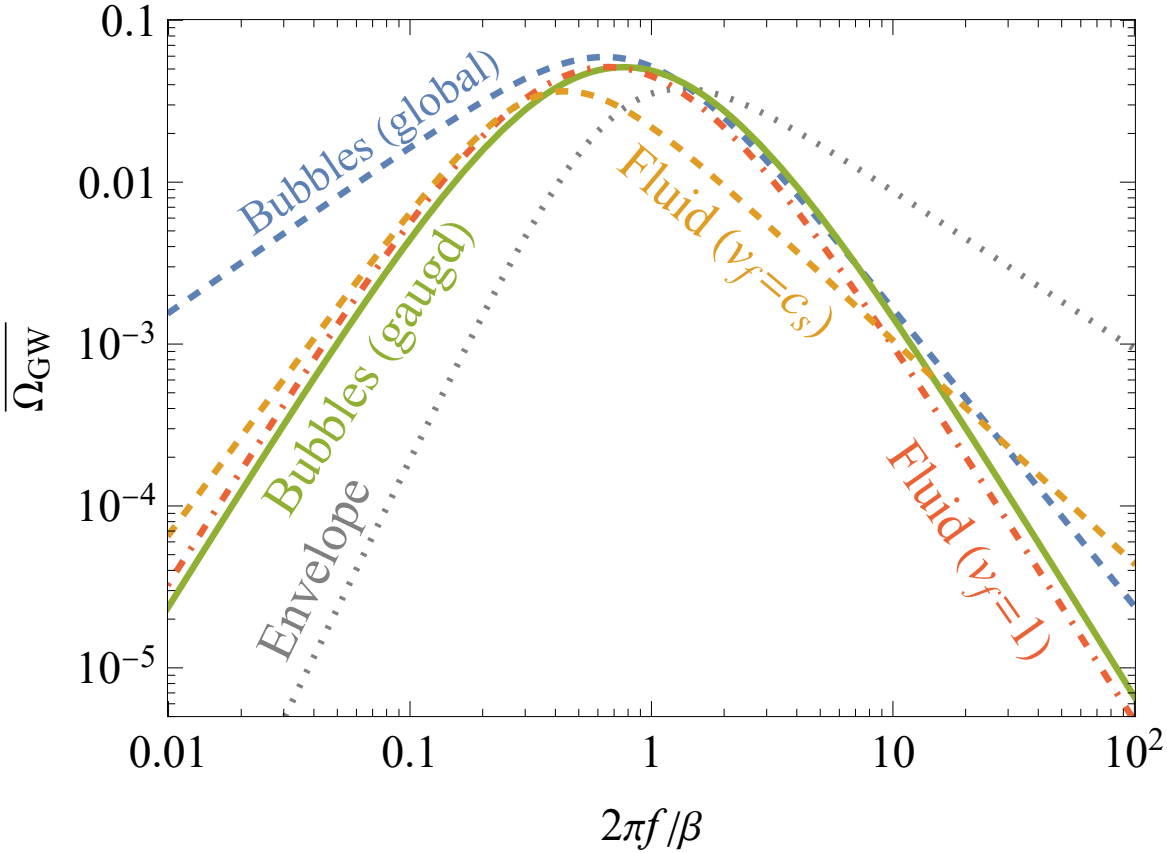

- Resulting spectrum:

$$\overline{\Omega_{GW}} = \frac{A\,(a+b)^c}{\left[b\left(\frac{f}{f_p}\right)^{-\frac{a}{c}} + a\left(\frac{f}{f_p}\right)^{\frac{b}{c}}\right]^c}$$

	Bubbles		Fluid
	Global($T \propto R^{-2}$)	Gauged ($T \propto R^{-3}$)	$v_{\rm shell} = 1$
$100\,A$	5.93 ± 0.05	5.13 ± 0.05	5.14 ± 0.04
a	1.03 ± 0.04	2.41 ± 0.10	2.36 ± 0.09
b	1.84 ± 0.17	2.42 ± 0.11	2.36 ± 0.09
c	1.91 ± 0.29	1.45 ± 0.34	3.69 ± 0.48
$2\pi f_p/\beta$	1.33 ± 0.19	0.64 ± 0.09	0.66 ± 0.04

ML, Ville Vaskonen arXiv: 2208.11697
ML, Ville Vaskonen, arXiv: 2007.04967

- Spectrum today

$$\Omega_{\rm GW}(f,T_*)h^2 \approx 1.6\times 10^{-5} S_H(f,f_H(T_*)) \left[\frac{\beta}{H}\right]^2 \frac{A(a+b)^c}{\left(b\left[\frac{f}{f_p}\right]^{-\frac{a}{c}} + a\left[\frac{f}{f_p}\right]^{\frac{b}{c}}\right)^c}$$

- Superhorizon modes

Gabriele Franciolini, Davide Racco, Fabrizio Rompineve arXiv: 2306.17136

$$f_H(T) = \frac{a(T)}{a_0}\frac{H(T)}{2\pi}\,, \quad S_H(f,f_H) = \left(1+\left[\frac{\Omega_{\rm CT}(f)}{\Omega_{\rm CT}(f_H)}\right]^{-\frac{1}{\delta}}\left[\frac{f}{f_H}\right]^{\frac{a}{\delta}}\right)^{-\delta}$$

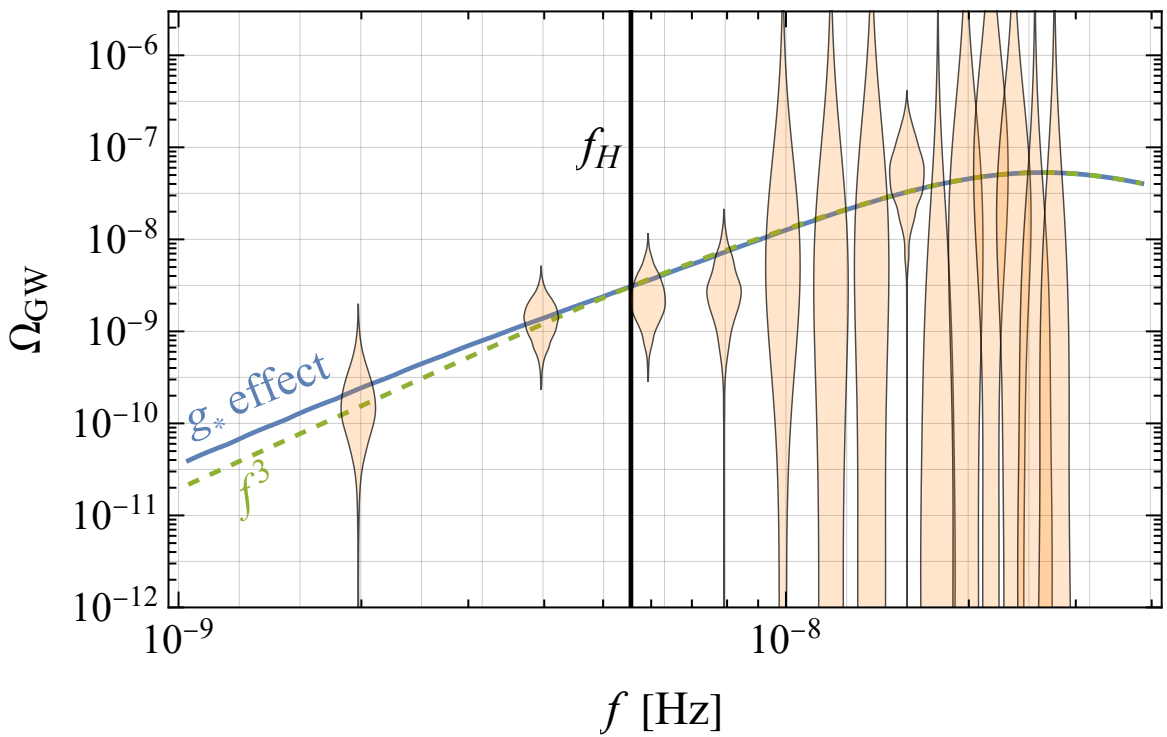

Fit to NANOGrav

- Constraint from PBH overproduction $\beta/H \gtrsim 3.9$
  ML, Piotr Toczek, Ville Vaskonen arXiv: 2305.04924

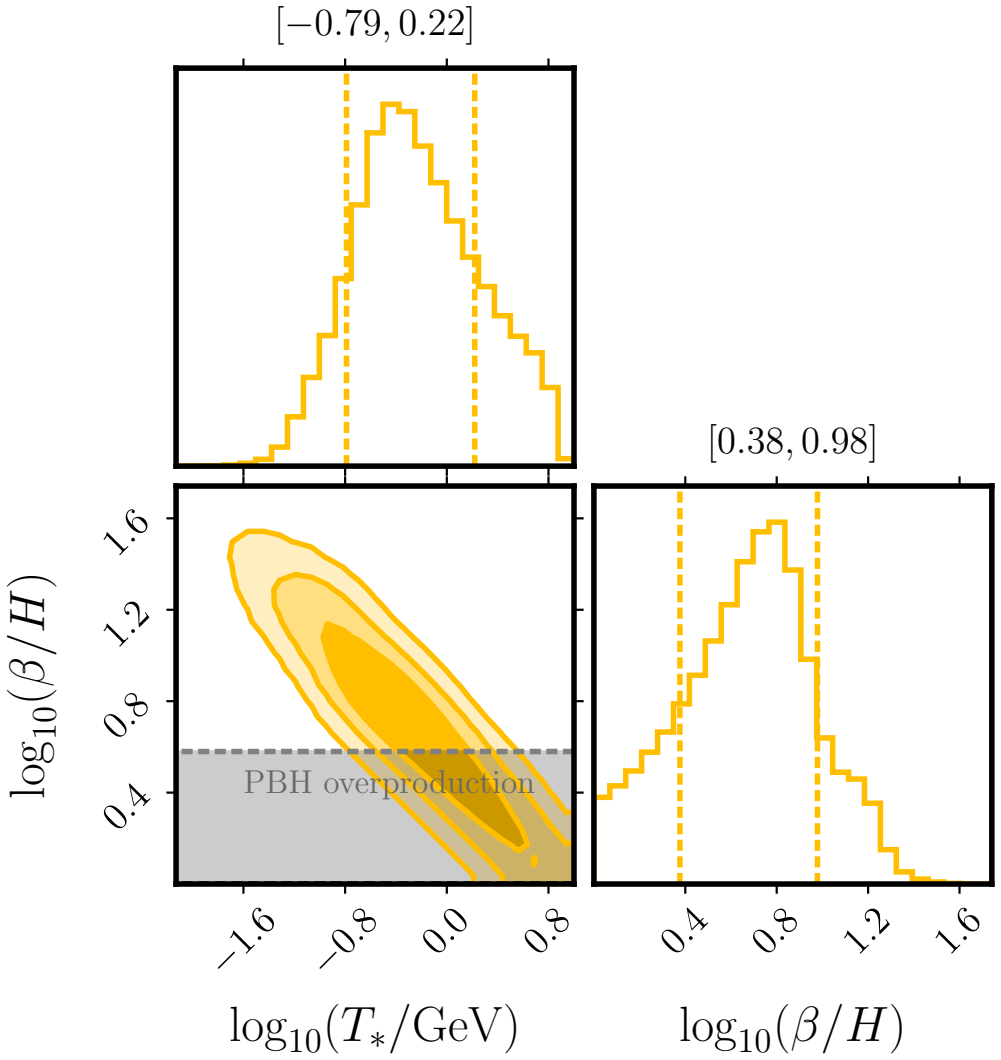

John Ellis et al. arXiv: 2308.08546

Results from Multi-Model Analysis (MMA)

Scenario	Best-fit parameters	ΔBIC
GW-driven SMBH binaries	$p_{\rm BH} = 0.25$	6.0
GW + environment-driven SMBH binaries	$p_{\rm BH} = 1$, $\alpha = 3.8$ $f_{\rm ref} = 12$ nHz	(BIC = 53.9)
Cosmic (super)strings	$G\mu = 2 \times 10^{-12}$, $p = 6.3 \times 10^{-3}$	-1.2
Phase transition	$T_* = 0.4$ GeV, $\beta/H = 5.5$	-4.9
Domain walls	$T_{\rm ann} = 0.79$ GeV, $\alpha_* = 0.026$	-5.7
Scalar-induced GWs	$k_* = 10^{7.6}$/Mpc $A = 0.08$, $\Delta = 0.28$	-2.1
First-order GWs	$\log_{10} r = -16$, $n_{\rm t} = 2.9$ $T_{\rm rh} = 0.35\,{\rm GeV}$	-2.0
"Audible" axions	$m_a = 3.1 \times 10^{-11}\,{\rm eV}$, $f_a = 0.87\,M_{\rm P}$	-4.2

For each model, we tabulate their best-fit values, and the Bayesian information criterion $BIC \equiv -2\Delta\ell + k \ln 14$ *relative to that for the purely SMBH model with environmental effects that we take as the baseline. The quantity in the parentheses in the third column shows the* ΔBIC *for the best-fit combined SMBH+cosmological scenario.*

Best Fits to NANOGrav including SMBH

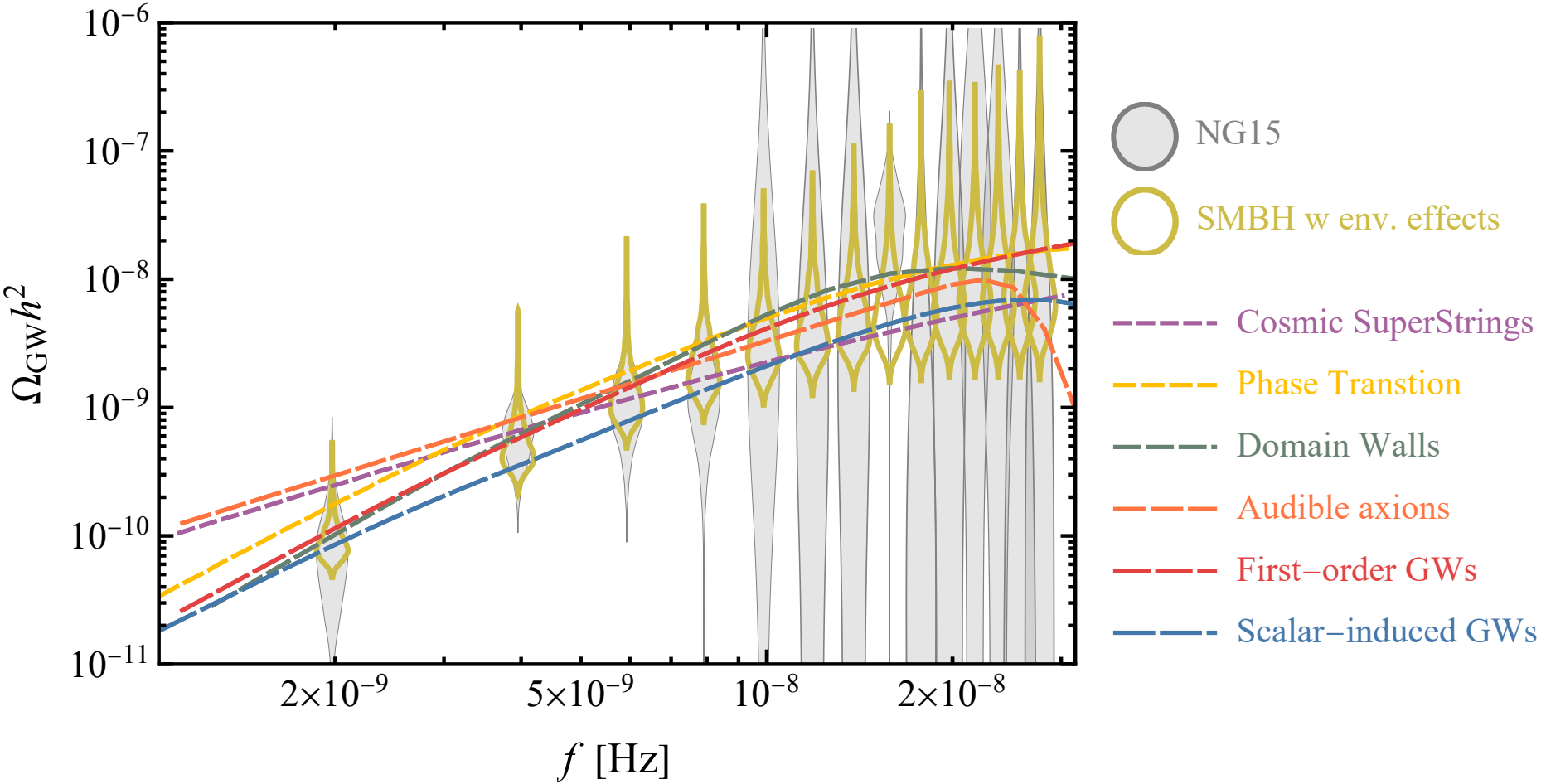

John Ellis et al. Phys.Rev.D 109 (2024) 2, 023522 arXiv: 2308.08546

Best Fits to NANOGrav including SMBH

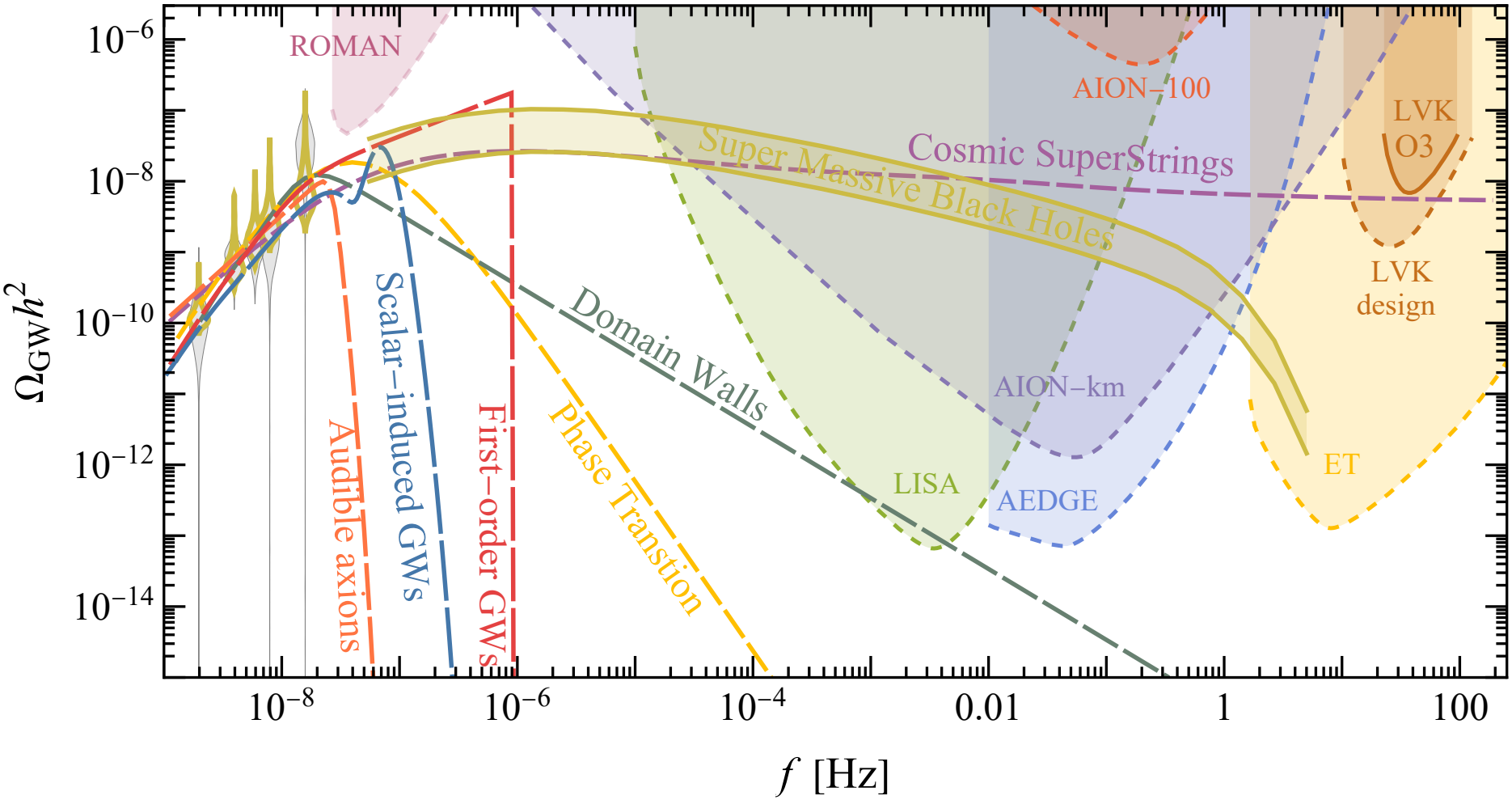

John Ellis et al. Phys.Rev.D 109 (2024) 2, 023522 arXiv: 2308.08546

Slow transitions produce PBHs

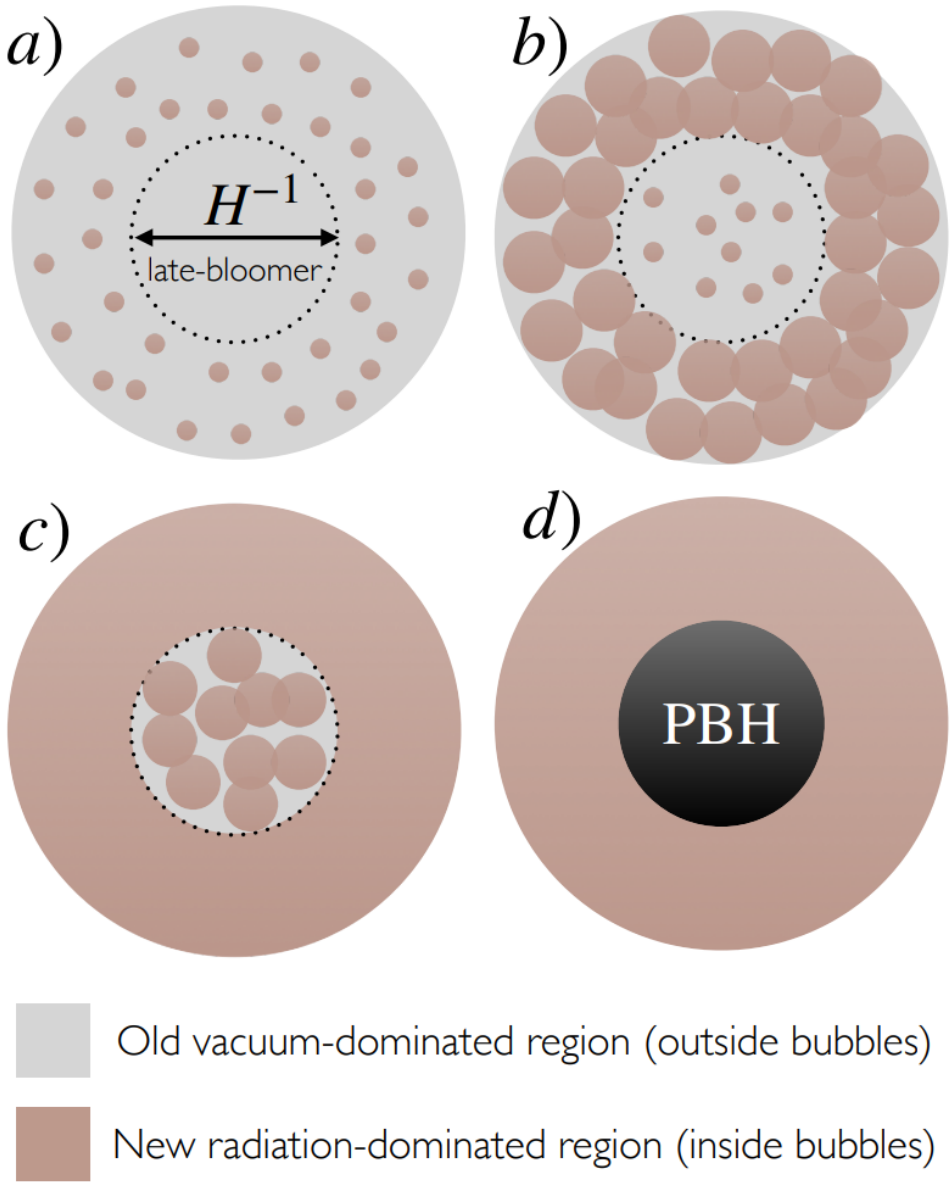

Yann Gouttenoire, Tomer Volansky, arXiv:2305.04942

Slow transitions produce PBHs

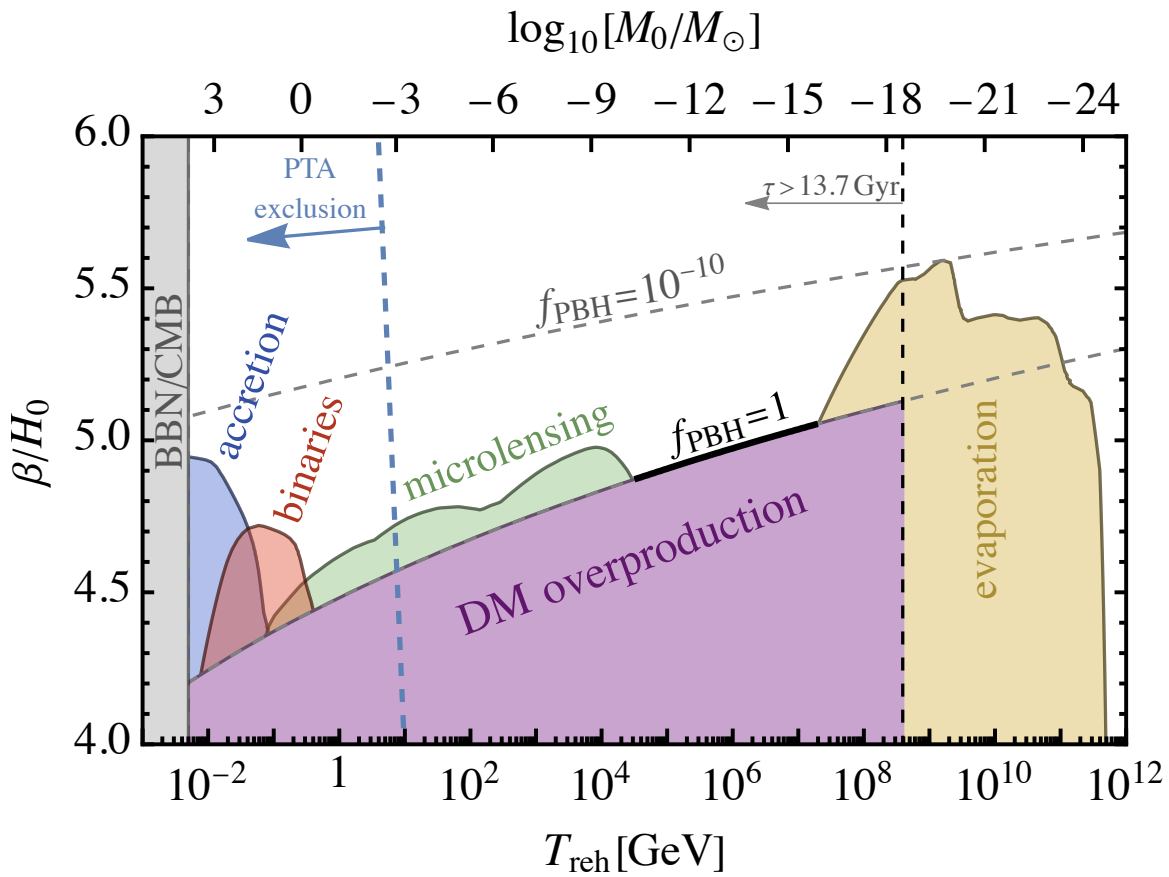

- Mass and abundance of PBHs

$$M_0 \approx 0.05 M_\odot \left[\frac{100}{g_*}\right]^{\frac{1}{2}} \left[\frac{T_{\mathrm{reh}}}{\mathrm{GeV}}\right]^{-2}, \quad f_{\mathrm{PBH}} = 2.8\times 10^9 \exp\left[-0.246 e^{\beta/H_0}\right] \frac{g_*}{g_{*s}} \frac{T_{\mathrm{reh}}}{\mathrm{GeV}}$$

ML, P. Toczek and V. Vaskonen, arXiv:2402.04158

Secondary GWs dominating for slow transitions

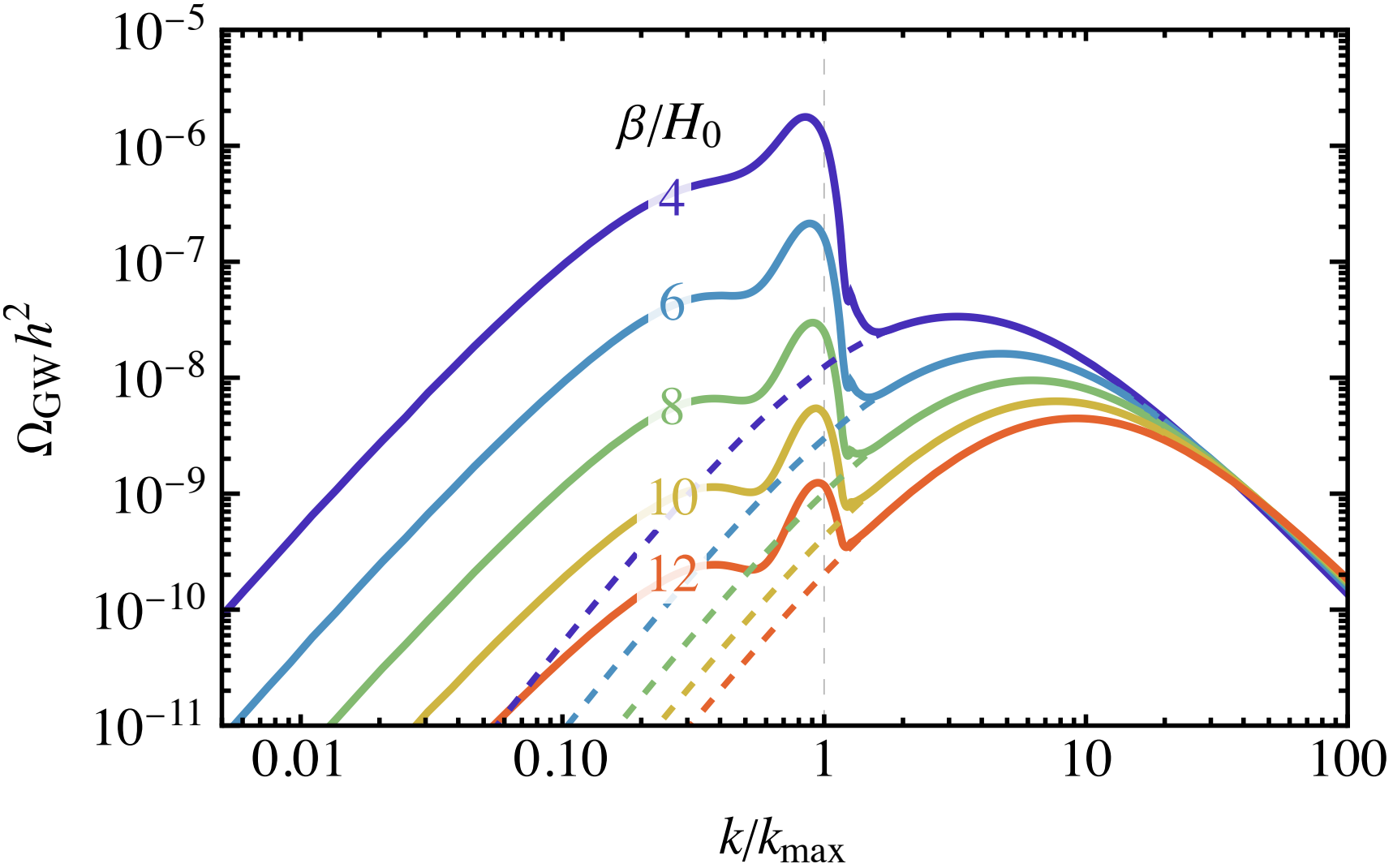

ML, P. Toczek and V. Vaskonen, arXiv:2402.04158

Secondary GWs: Impact on PTA fits

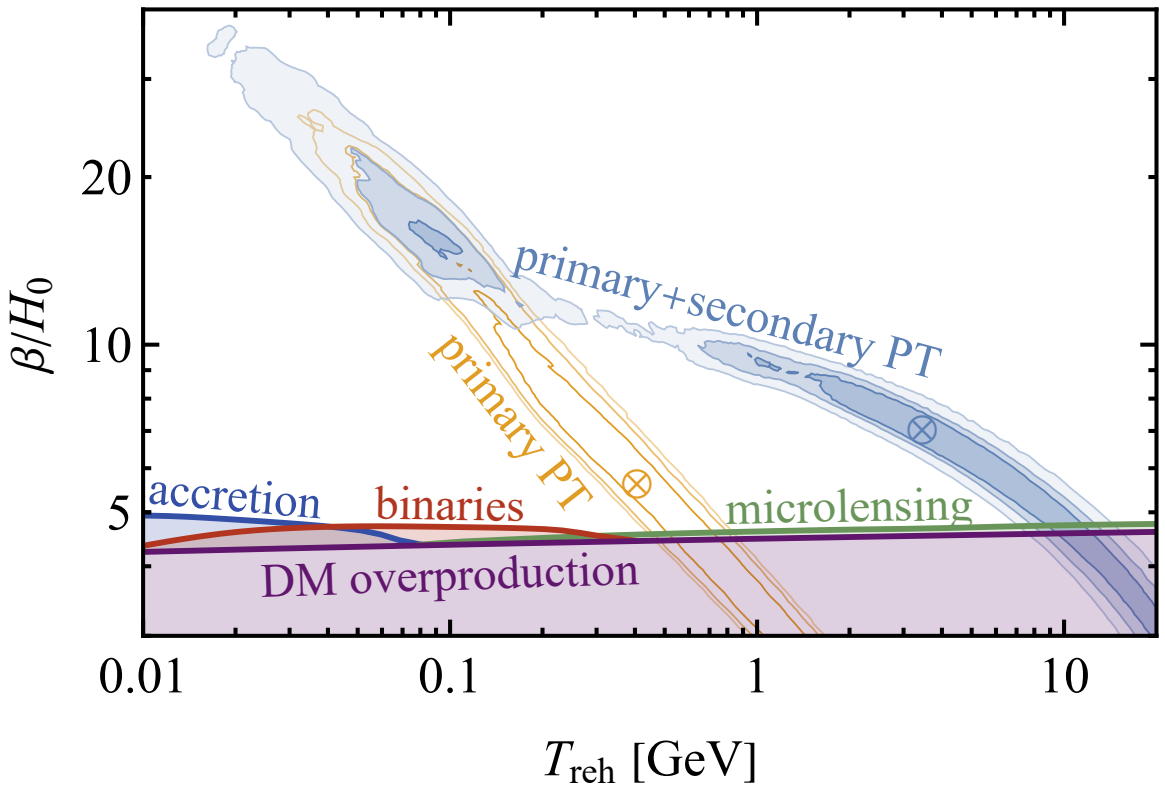

- Best fit with primary vs primary+secondary GWs

$T_{\rm reh} = 0.4\,\text{GeV}$ $\quad$ $T_{\rm reh} = 3.4\,\text{GeV}$

$\beta/H = 5.5$ $\quad$ $\beta/H = 7.0$

ML, P. Toczek and V. Vaskonen, arXiv:2402.04158

Secondary GWs: Detection prospects

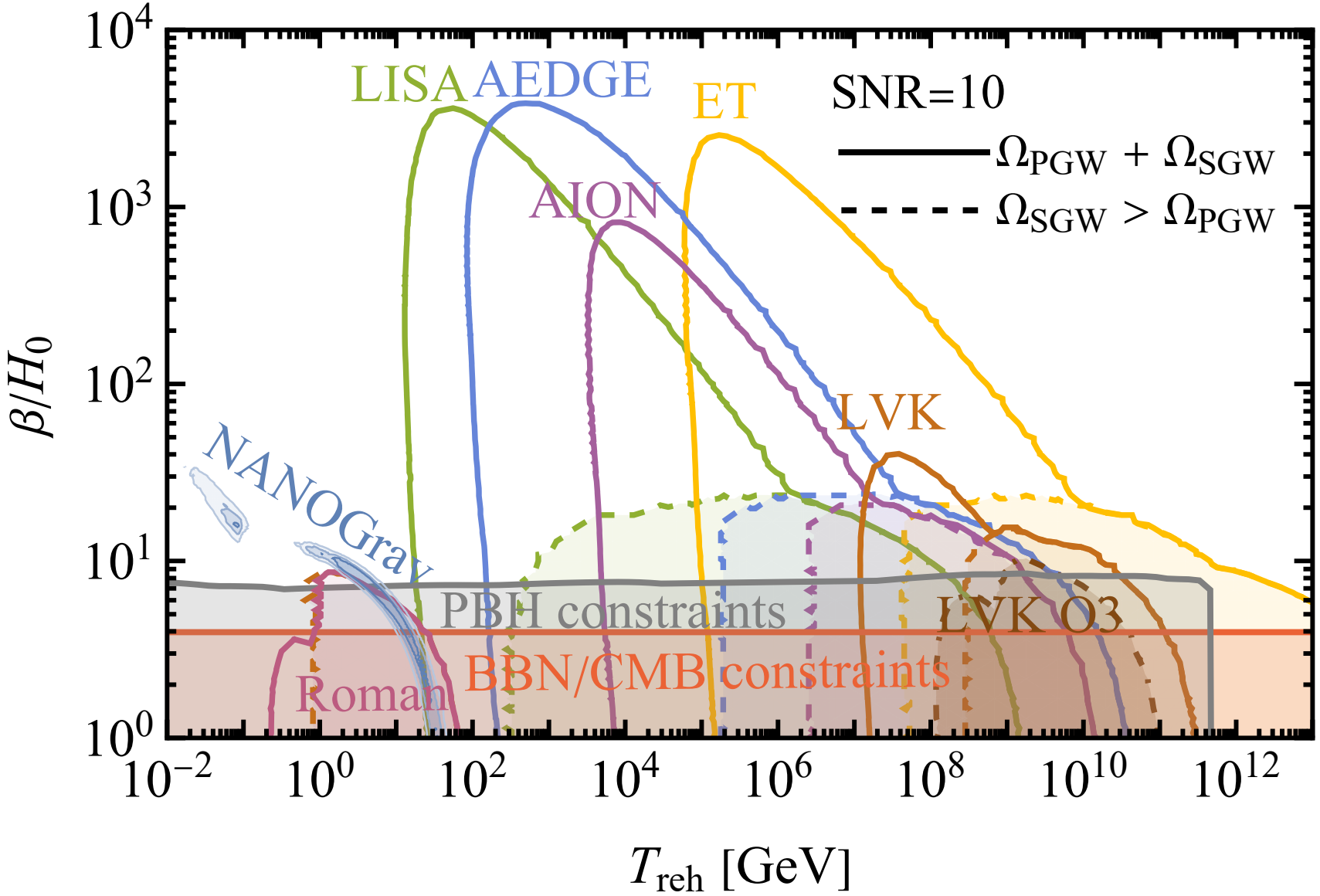

ML, P. Toczek and V. Vaskonen, arXiv:2402.04158

Theoretical uncertainty on the parameter space

- Standard Model with an additional singlet scalar

$$V(H,s) = -\mu_h^2|H|^2 + \lambda|H|^4 + \frac{\lambda_{hs}}{2}S^2|H|^2 + \left(m_s{}^2 - \frac{\lambda_{hs}v^2}{2}\right)\frac{s^2}{2} + \frac{\lambda_s}{4}S^4$$

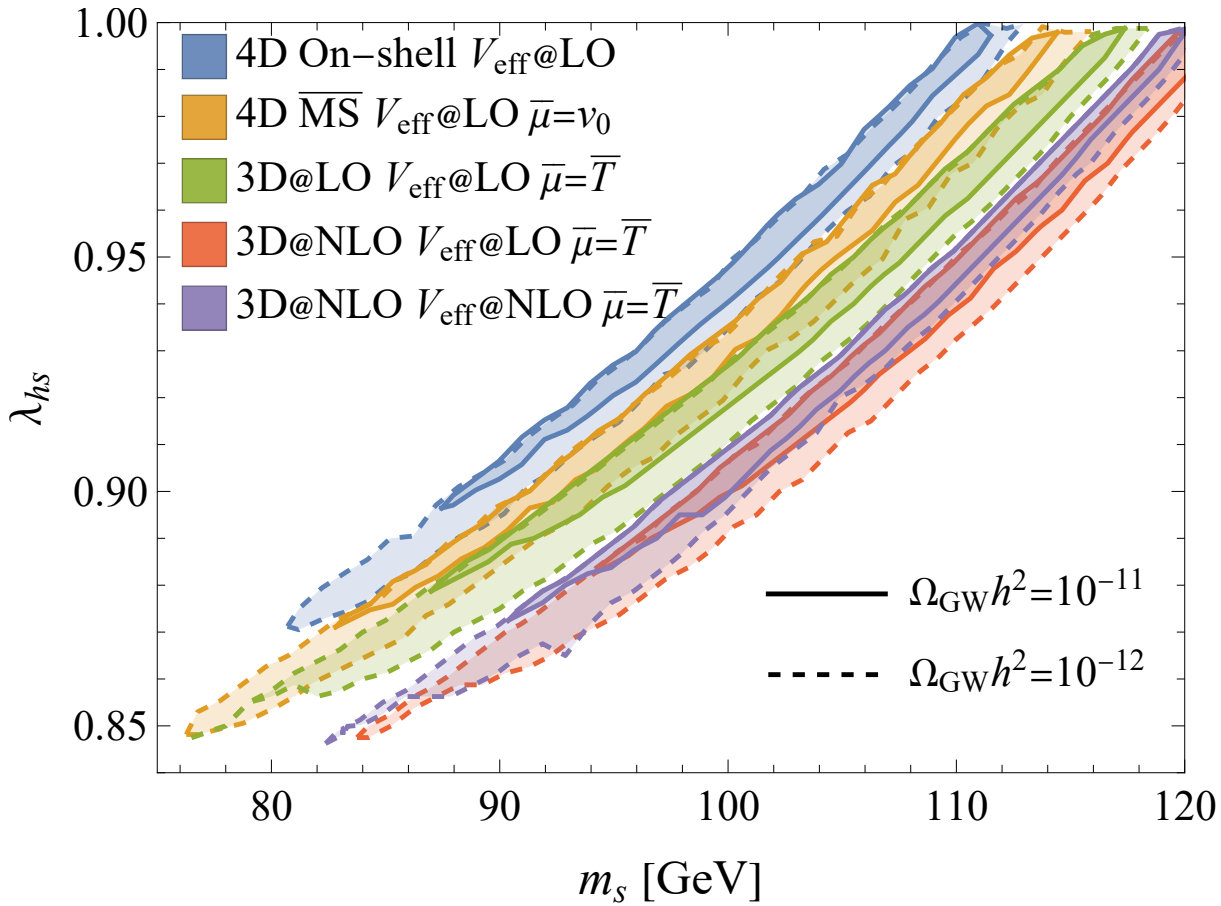

ML, Marco Merchand, Laura Sagunski, Philipp Schicho, Daniel Schmitt arXiv:2403.03769

Theoretical uncertainty on the parameter reconstruction

- Standard Model with an additional singlet scalar

$$V(H,s) = -\mu_h^2|H|^2 + \lambda|H|^4 + \frac{\lambda_{hs}}{2}S^2|H|^2 + \left(m_s{}^2 - \frac{\lambda_{hs}v^2}{2}\right)\frac{s^2}{2} + \frac{\lambda_s}{4}S^4$$

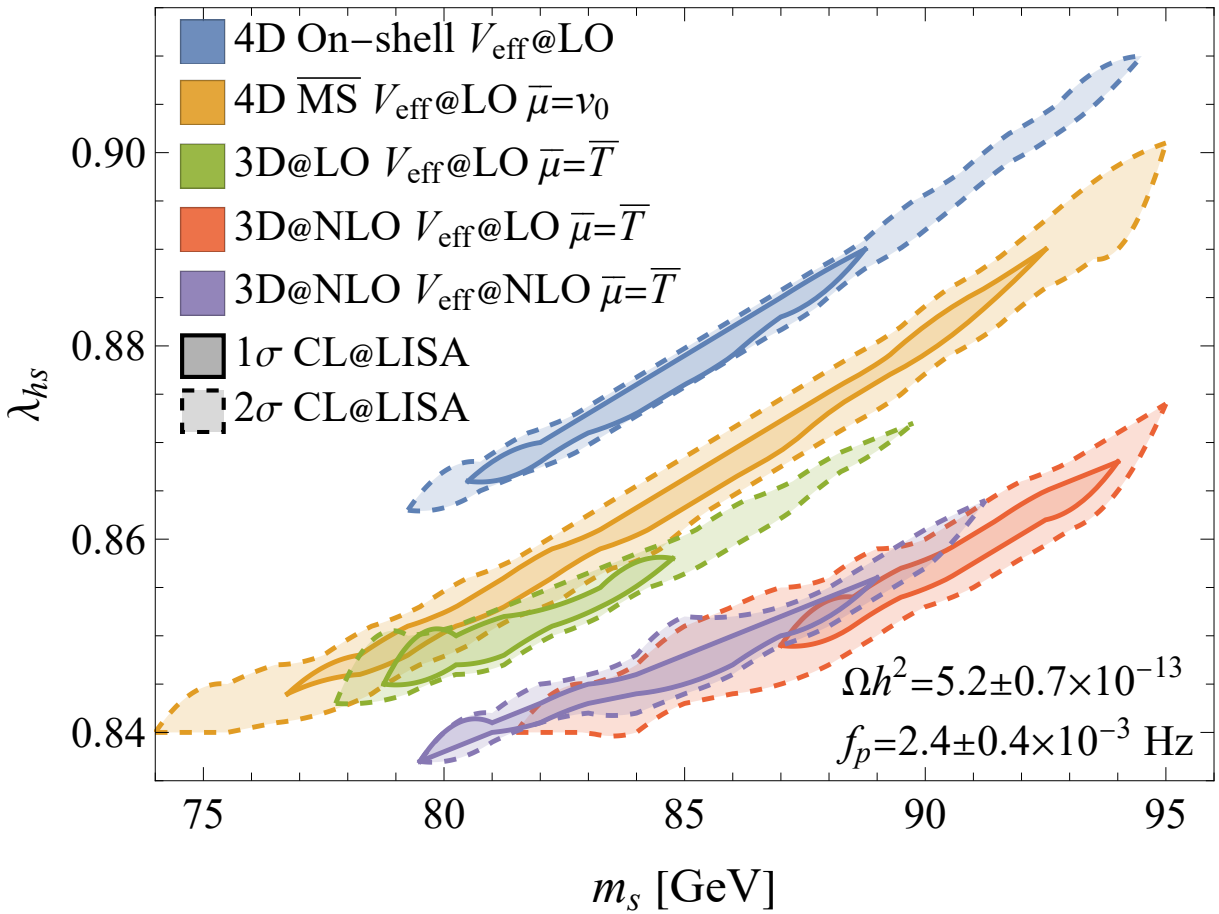

ML, Marco Merchand, Laura Sagunski, Philipp Schicho, Daniel Schmitt arXiv:2403.03769

Theoretical uncertainty on the parameter space

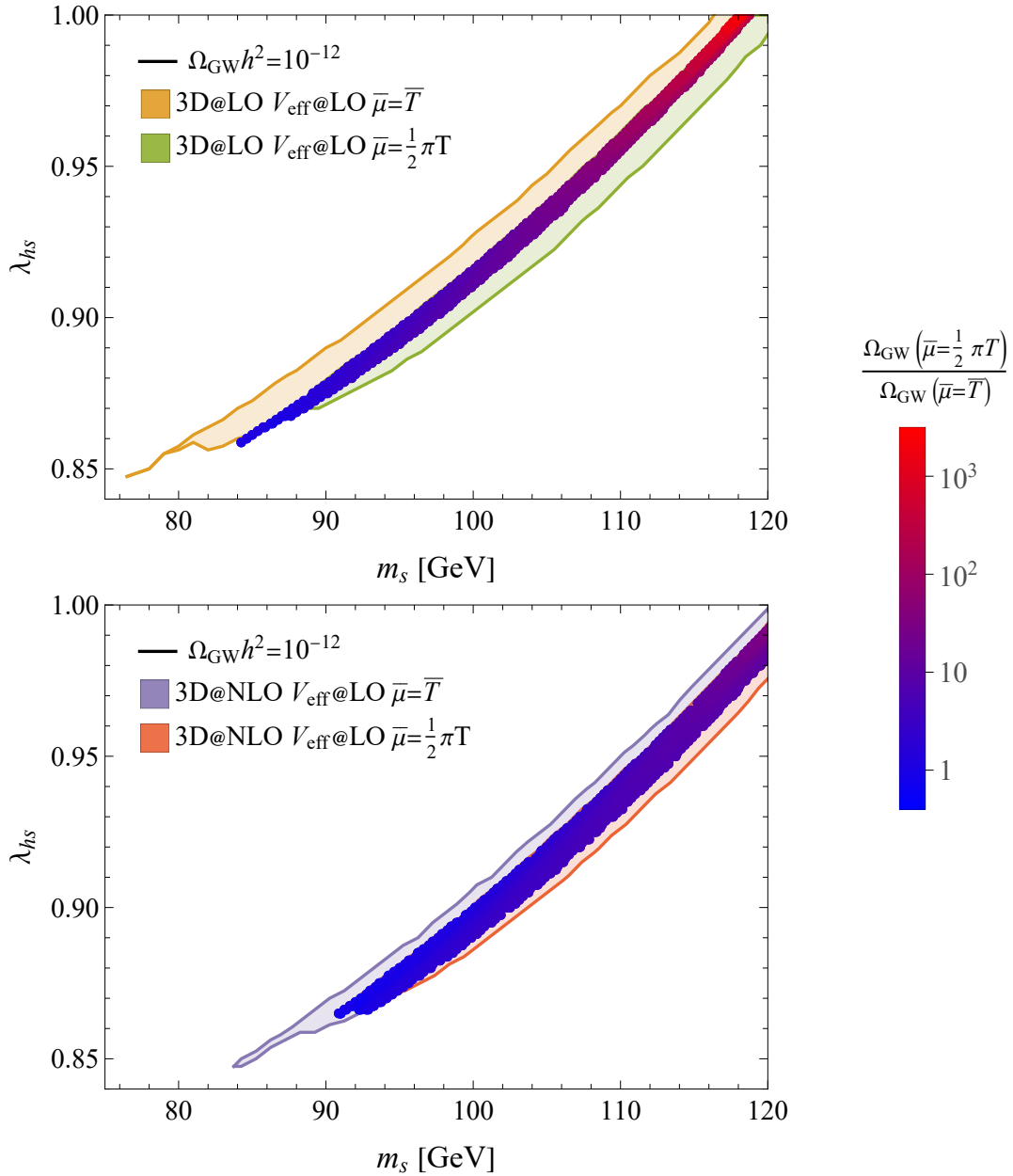

ML, Marco Merchand, Laura Sagunski, Philipp Schicho, Daniel Schmitt arXiv:2403.03769

Conclusions

- Very strong transitions ($\alpha \gg 1$) produce the same GW spectrum regardless of whether the main source is collisions of bubble or motion of the plasma.
- A very strong phase transition is one of the best explanations for the current PTA data.
- If the transition is also slow ($\beta/H \lesssim 10$) a secondary GW contribution will dominate the spectrum and a large population of PBH can be created.
- Large errors on the GW spectra for individual parameter points corresponds to small $O(1\%)$ error on the reconstructed model parameters
- These small reconstruction errors would still dominate the experimental uncertainties for any detectable spectra

Thank you for your attention!